Erasmus MC
Universitair Medisch Centrum Rotterdam

ICIN

Thoraxcentre

The Eleventh European Symposium on Ultrasound Contrast Imaging

Folkert J. Ten Cate, MD
Nico de Jong, PhD
M.J.K. Blomley, MD

Abstract book

January 26-27, 2006, Rotterdam, The Netherlands

11th EUROPEAN SYMPOSIUM ON ULTRASOUND CONTRAST IMAGING
26-27 JANUARY 2006, Rotterdam, The Netherlands

WEDNESDAY, 25 January 2006

18.00 - 20.00 **Registration - Welcome Drinks - Posters** ..... **Hilton Hotel**

THURSDAY, 26 January 2006

08.00 - 09.00 **Registration**

09:00 - 09:05 **Opening by Prof.dr. M.L. Simoons, head of the department of Cardiology**

9.05 - 10.35 **CLINICAL APPLICATIONS** ..... *Chairpersons:Otto Kamp and Folkert ten Cate*

Mark Monaghan — Something to do with 3D and Contrast. Probably Contrast 3D post MI remodelling **1**
Harald Becher — Myocardial Contrast Echocardiography what can we learn from MRI and SPECT **4**
Roxy Senior — Myocardial contrast echocardiography in Clinical Practice or as suggested by the directors **5**
Jean-Michel Correas — Contrast-enhanced ultrasound of the thyroid **6**
Thomas Fischer — Contrast-enhanced US in renal transplant: first results and potential clinical benefit **8**

10.35 - 11.00 **Intermission**

11.00 - 12.30 **TECHNOLOGY I** ..... *Chairpersons: Nico de Jong and Michel Versluis*

Mark Borden — Physicochemical Properties of Targeted Microbubble Shells **9**
Marcel Böhmer — Preparation and Characterization of Monodisperse Polymer-shelled Ultrasound Contrast Agents **10**
Jeroen Sijl — Acoustical study of the properties of single/individual phospholipid-based ultrasound contrast agent Microbubbles..... **13**
Paul Prentice — Experimental Observation of Cell Membrane Rupture by Microbubble Cavitation **15**
Jim Chomas — New Ultrasound Imaging Method for Molecular Imaging **17**

12.30 – 14.00 **LUNCH**

14.00 - 14.45 **ICIN*-Lecture** ..... *Chairperson: Nico de Jong*

Peter Burns — Imaging Tumour Angiogenesis with Ultrasound **19**

14.45 – 16.00 **BIOMARKERS** ..... *Chairpersons: Tom Porter and Jeff Powers*

Ferdinand Frauscher — Imaging of prostate using contrast **22**
Raffi Bekeradjian — New developments in therapeutic applications of microbubbles **23**
Annemieke van Wamel — Ultrasound contrast agent mediated temporal adjusted vascular permeability. **24**
Piotr Lipiec — Myocardial contrast enhancement with real-time time imaging allows accurate assessment of myocardial perfusion and improves the diagnostic value of standard stress echocardiography **26**

16.00 – 16.30 **Intermission**

16.30 – 17.45 **ATHEROSCLEROSIS** ..... *Chairpersons: Roxy Senior and Annemieke van Wamel*

Dave Goertz — Contrast Intravascular Ultrasound: Progress Towards Coronary Artery Vasa Vasorum Imaging . **28**
Steve Feinstein — Atherosclerosis imaging of carotids arteries **30**
Jonathan Lindner — Molecular Imaging of Angiogenesis **31**
Sarah Taylor — Highly-Targeted Retroviral Gene Delivery Using Ultrasound. **33**

18.30 - 22.30 **SOCIAL EVENT (Incl. Dinner buffet)** **87**

*** ICIN = The Interuniversity Cardiology Institute of the Netherlands**

FRIDAY, 27 January 2006

07.30 - 08.00 **Registration**

07.30 - 09.00 **POSTER DISCUSSION A** ……..*Moderator: Folkert ten Cate*

The best clinical poster price is sponsored by Nycomed

07.30 - 09.00 **POSTER DISCUSSION B** .....*Moderator: Nico de Jong*

The best technical poster price is sponsored by SUGB
(the Dutch Foundation for Ultrasound Society in Medicine &Biology)

FRIDAY, 27 January 2006

Announcement of the winners of the poster-prices by Jonathan Lindner and Ton van der Steen

REAL-TIME 3D ECHO: A COMPARISON WITH STATE OF THE ART 2D IMAGING

Dr. Stamatis Kapetanakis, MBBS, MRCP King's College Hospital London, SE5 9RS, UK
Mr. David S. Mullins, BSc (Hons) King's College Hospital London, SE5 9RS, UK
Dr. George Amin, MBBS, MRCP King's College Hospital London, SE5 9RS, UK
Dr. Penelope Giannakopoulou Queen Elizabeth Hospital London, SE18 4QH, UK
Dr. Mark J. Monaghan, PhD, FESC King's College Hospital London, SE5 9RS, UK

Background

Real-Time 3D Echocardiography (RT3DE) is a recently introduced imaging modality which provides three-dimensional volume rendering of cardiac structures as easily as conventional 2D echocardiography. RT3DE has been shown to be more accurate than 2D imaging in quantification of LV volume, mass and function, as frequently the long axis planes are foreshortened in the latter. As with any transthoracic approach however, RT3DE is subject to the same artefacts as 2D imaging. Ultrasound contrast has successfully been used to enhance endocardial border detection in conventional 2D echocardiography. We investigated the feasibility and value of ultrasound contrast in RT3DE

Methods

50 unselected patients attending for routine dobutamine stress echocardiography (DSE) were recruited. 2D and RT3D echocardiography was performed with the Sonos 5500 and 7500 respectively. 2D imaging was performed with power-modulation (Mechnical Index 0.1) and continuous infusion of SonoVue® (0.8 mł/min) at baseline, low, intermediate and peak stress. RT3DE was performed with and without contrast at baseline and at peak stress with low mechanical index (MI 0.3) and continuous infusion of SonoVue® (1 mł/min). 3D images were cropped to resemble the 4 standard 2D views (apical 4-, 2-and 3-chamber views and a short axis view at papillary level).

Each digital loop was scored for image quality on a 4-point scale (0 = not interpretable, 1 = limited image quality, 2 = adequate image quality and 3 = excellent image quality). "Not interpretable" was assigned to loops with fewer than 3 of 6 visible segments and "limited visualisation" was assigned to loops with fewer than 5 of 6 segments visible. Each segment was scored for endocardial definition on a 3 point scale (0 = not visualised, 1 = limited visualisation and 2 = adequate visualisation). "Limited visualisation" was assigned to segments either partially visible, or visible during only a portion of the cardiac cycle. An Endocardial Border Definition Index (EBDI) was defined as the average score for endocardial definition in each loop (range 0 -2, higher is better). Wall motion was assessed with the Wall Motion Score Index as previously described.

Results

The average acquisition time for RT3DE was 25±5 sec and had an average frame rate of 19.5±0.5 Hz. 39 patients were examined at peak stress. The remaining 11 did not undergo RT3DE in addition to the 2D on clinical grounds. No 2D DSEs were performed without contrast. 30 patients were male and 20 were female with an average age of 62.5 years (range: 39 – 84 years). All patients were adults with known or suspected coronary artery disease.

Endocardial Definition

At baseline, there was a statistically significant improvement in image quality with contrast enhancement. Many more video loops had adequate (59% of contrast images vs. 36.25% of non contrast images) or excellent (28.2% of contrast images vs. 8.5% of non contrast images) image quality. Significantly fewer loops were considered "not interpretable" when enhanced with contrast (0.75% vs. 18.3% of non contrast images, $p<0.001$ for all comparisons). The EBDI for RT3DE increased significantly with contrast administration (1.87±0.29 vs. 1.09±0.6, $p < 0.001$). At peak stress there was a non-significant reduction in image quality (image quality score 1.92±0.84 vs. 2.15±0.64, $p = 0.08$). There was also a nonsignificant reduction in EBDI (1.5±0.48 vs. 1.87±0.29, $p = 0.1$).

Assessment of Regional Wall Motion

There was an excellent correlation between WMSI in 2D and RT3DE contrast-enhanced loops at baseline ($R = 0.963$, $p<0.0001$). The Bland-Altman excellent agreement with average difference of 2D-3D WMSI of 0.004±0.12. This correlation was maintained at peak stress ($R = 0.969$, $p<0.0001$). Bland-Altman analysis demonstrated a slight reduction in agreement between 2D and RT3D WMSI at peak stress (mean difference -0.01±0.16).

Discussion

Real-time 3D echocardiography offers many potential benefits over two-dimensional imaging. The RT3D data set can produce any view of the left ventricle, minimising errors due to foreshortened views and accommodating less experience operators. The datasets can be obtained and displayed within a few seconds

making this method clinically relevant, particularly for modalities such as stress echocardiography. In this study, a significant proportion of patients had suboptimal imaging with real-time 3D echo with regards to assessment of LV function (55%), although only a small percentage had images classed as "not interpretable". In part, this is due to the fact that fundamental imaging was used in the non-contrast echoes – the implementation of harmonic imaging in the X4 matrix array transducer produces suboptimal results with non-enhanced 3D images. A continuous infusion of echo contrast during 3D harmonic imaging produced a significant improvement in endocardial border definition and image quality. At peak stress, a reduction in both image quality score and EBDI was noted, which may be in part due to higher rate of contrast destruction (small LV cavity). With contrast-specific acquisition settings, apical contrast destruction was minimised in most cases at both rest and stress, although was present to some degree in approximately two-thirds of patients. The effect of this was further minimised with image post-processing. Importantly, there was an excellent correlation between 2D and RT3D wall motion interpretation at both rest and peak stress.

Conclusions

Contrast enhanced real-time 3D echocardiography is feasible in all patients referred for assessment for assessment of left ventricular function and significantly enhances endocardial border delineation and image quality. Short acquisition times and independence from off-axis acquisition errors make this a clinically useful modality, and may be particularly useful during stress echocardiography.

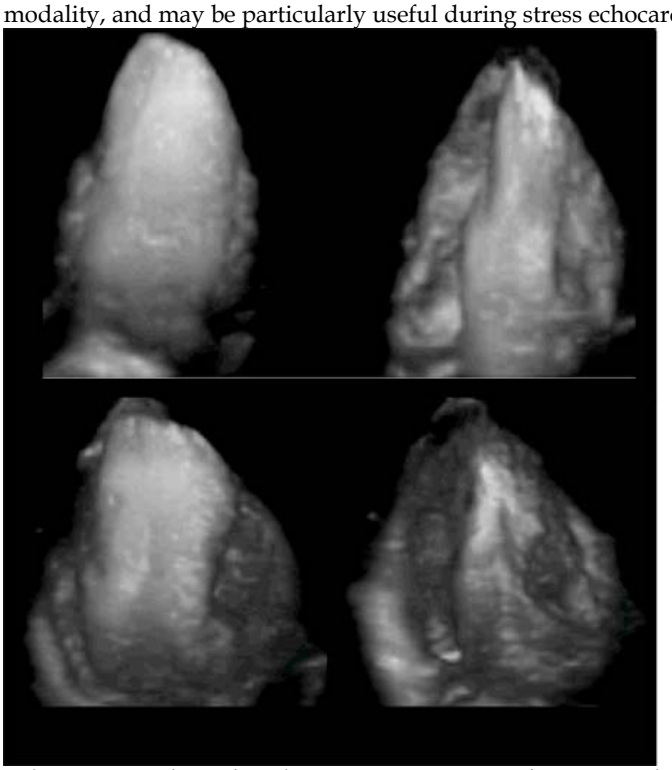

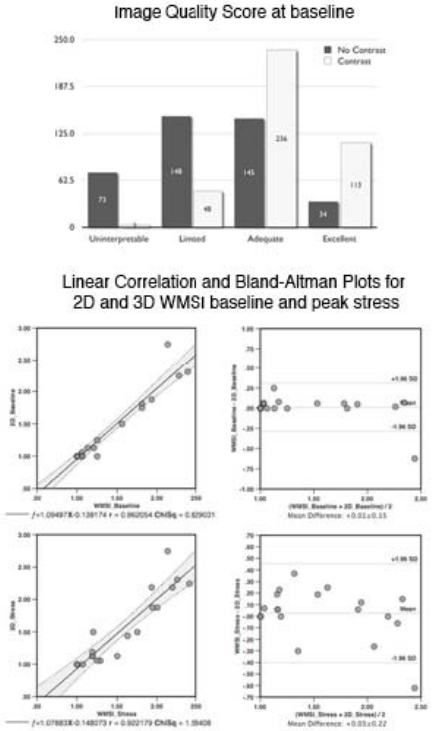

Left: Contrast enhanced Real-Time 3D image cropped to an apical 4-Chamber view in end-diastole (top) and end-systole (bottom). **Right:** Image quality score at baseline with and without contrast-enhancement (top). Linear correlation and Bland-Altman plots for WMSI in 2D vs. 3D and baseline (mid) and peak stress (bottom).

A Myocardial Contrast Echocardiography
Can we lean from other imaging modalities?

Harald Becher

John Radcliffe Hospital Oxford, UK

In the future myocardial perfusion imaging can be performed with 3 different imaging modalities: myocardial scintigraphy, magnetic resonance tomography (MRI) and myocardial contrast echocardiography. In particular myocardial scintigraphy has been successful for a long time because of several practical issues, which are worth to be considered for myocardial contrast echocardiography:

1. Data acquisition has to be completely standardized and simplified. This has been achieved for LVO studies already (Thibault H, JASE 2005)
2. Minimize physicians time: Insertion of IV lines and image acquisition can be performed by nurses and/or technicians. Like in stress ECG a physician should be in the department but does not need to attend.
3. Short stress protocols (vasodilator) to limit the number of recordings and time per patient
4. Postprocessing – if necessary – by technicians
5. Reporting according to the needs of the clinicians (normal, presence and extent of reversible ischaemia or scar)
6. Large data base for outcome like myocardial scinitgraphy

Assessment of myocardial perfusion by myocardial contrast echocardiography – An innovative technique

Roxy Senior MD, DM, FRCP, FESC, FACC

Department of Cardiovascular Medicine, Northwick Park Hospital, Harrow, Middlesex, UK

A constant search continues in the practice of cardiology to determine the "ideal" imaging modality that could evaluate cardiac structure, function and perfusion. Recent advancements in the field of echocardiography have resulted in simultaneous improvements in both techniques and image quality permitting echocardiography to maintain its position as the primary non-invasive imaging modality. In particular, the development of newer ultrasound contrast agents and advances in imaging techniques have now made possible the assessment of myocardial perfusion. Myocardial contrast echocardiography (MCE) utilises acoustically active gas filled microspheres (microbubbles) which have rheology similar to that of red blood cells. The detection of myocardial perfusion during echocardiographic examinations permits simultaneous assessment of global and regional myocardial structure, function, and perfusion, enabling optimal non-invasive assessment of coronary artery disease. In future, its use will not be limited solely to diagnostic assessment. MCE has the potential for therapeutic delivery of growth factors, genes and aiding thrombolysis. MCE has evolved from the experimental laboratory to daily clinical practice for the bedside evaluation of ischaemic heart disease.

KEY WORDS:

Myocardial contrast echocardiography

Acute myocardial infarction

Myocardial blood volume

Coronary artery disease

Microbubbles

Single photon emission computed tomography

Contrast-enhanced ultrasonography of the thyroid : preliminary results

JM Correas, H Montpeyssen, J Tramalloni, O Hélénon

Department of Adult Radiology, Necker University Hospital, Paris, France

Current indications of ultrasound contrast agents (USCAs) are extending to new areas, and particularly to the assessment of superficial tissues. This move can be attributed to the introduction of USCAs with strong resonant properties at low acoustic power and imaging techniques with higher sensitivity.

In Europe, SonoVue® (Bracco, Italy) has become widely available and exhibits a good safety profile in routine radiological practice. The approved dosage of 2.4 mL allows real time enhancement of parenchymal micro and macrovasculature using broadband curvilinear transducers (from 1 to 6 MHz). The most targeted organ remains the liver, for the characterization and the detection of focal liver diseases. Out of the approved indications, the characterization of solid tumors in the kidney is disappointing due to the lack of specific pattern. US imaging modalities for the detection of microbubbles improved during the past 5 years and have become available on linear transducers of higher frequency (4 to 8 MHz). Among these modalities, CPS (Cadence Contrast Pulse Sequencing; Acuson-Siemens; USA), Pulse inversion imaging (Philips US, USA) and VRI (Vascular Recognition Imaging, Toshiba, Japan) can be used to study the thyroid after USCA administration. Previous study of thyroid nodules with USCAs was performed using color and power Doppler imaging. The analysis of time intensity curves obtained after Levovist® injection using Power Doppler imaging during the wash out phase was helpful in order to differentiate benign vs malignant nodules. Argalia et coll. found that benign lesions exhibited a monophasic wash-out curve in 93% of the cases while 89% of malignant nodules had a polyphasic wash-out curve.

The purpose of our pilot study was to evaluate the value of real-time contrast-enhanced US (CE-US) for the characterization of thyroid nodules with suspicious characteristics of cancer at baseline US. Fourteen patients (12 women, 2 men) were studied using a high frequency linear transducer (L12-5) on a HDI 5000 (Philips US, Bothell, USA). After signing the informed consent form, the contrast-enhanced US examination was performed at low mechanical index using real time pulse inversion after the administration of a bolus injection of SonoVue®. Microvascular imaging was systematically used at the end of the microbubble transit in the thyroid. The kinetics of the USCA was analyzed using HDILab® (Philips US, Bothell, USA) in linear mode. One ROI was positioned upon the nodule; the other one was set at the same depth in the normal thyroid parenchyma. The radiologist was blinded to any biological and histological results. Results were correlated to fine needle aspiration in benign lesions and to both fine needle aspiration and histology in cancers. A total of of 16 nodules was studied with 8 malignant lesions corresponding to papillary tumors (5) and vesicular lesions (3).

Contrast enhancement was consistently observed at the level of the nodule and the normal thyroid parenchyma. The thyroid gland enhanced 5 to 8 sec after the bolus administration of SonoVue®. Peak enhancement was delayed and higher in malignant lesions without any statistically significant difference to benign lesions, possibly due to the limited number of cases. Average peak enhancement was found at 5.7 sec (min 5 sec; max 8 sec) in the normal gland and at 7.8 sec (min 6.8; max 10 sec) in malignant lesions. Peak enhancement was ranging from 13 to 16 dB in normal thyroid and 12 to 15 dB in malignant lesions. Benign nodules exhibited a hypervascular rim covering at least 50% of the border. Malignant lesions were correctly identified in all cases due to the desorganization of the vascularity. Malignant criteria at CE-US were: 1) a moderate enhancement inferior to that of the normal surrounding parenchyma without continuous hypervascular peripheral rim 2) the heterogeneity of the enhancement within the nodule 3) the presence of necrotic areas. In one case, CE-US classified the nodule as benign while fine needle aspiration was showing element of malignancy. However, histology following thyroidectomy confirmed the absence of malignancy.

Despite the limited number of cases, CE-US of the thyroid using SonoVue® appeared as a valuable technique in order to differentiate benign and malignant lesions. Multicenter clinical trials are now required to evaluate the real performance of this new imaging modality.

Bibliography

Argalia G, De Bernardis S, Mariani D, Abbattista T, Taccaliti A, Ricciardelli L, Faragona S, Gusella PM, Giuseppetti GM. Ultrasonographic contrast agent: evaluation of time-intensity curves in the characterisation of solitary thyroid nodules. Radiol Med (Torino). 2002 Apr;103(4):407-13.

Spiezia S, Farina R, Cerbone G, Assanti AP, Iovino V, Siciliani M, Lombardi G, Colao A. Analysis of color Doppler signal intensity variation after levovist injection: a new approach to the diagnosis of thyroid nodules. J Ultrasound Med. 2001 Mar;20(3):223-31.

Iannuccilli JD, Cronan JJ, Monchik JM. Risk for malignancy of thyroid nodules as assessed by sonographic criteria: the need for biopsy. J Ultrasound Med. 2004 Nov;23(11):1455-64.

Contrast-enhanced US in renal transplant: first results and potential clinical benefit

Thomas Fischer

Department of Radiology - University of Berlin – Germany

Purpose. Relying on the US contrast media (USCM) of the second generation and an improved US technology, we performed a study to investigate whether it is possible to adequately diagnose rejection after kidney transplant by evaluating the arterial inflow of an USCM.

Methods. So far, a total of 62 patients underwent US examination with an echo enhancer (1.6 ml SonoVue) 5 to 7 days after kidney transplantation. The examinations were performed using the Aplio US system (Toshiba) with a 3.5-MHz transducer and the technique of contrast harmonic imaging (MI 0.1). Contrast medium inflow was determined in the interlobar artery and the renal cortex by means of the US system's integrated time-intensity curve software. An acute rejection quotient (ARQ) was defined as the ratio of the slopes of the USCM inflow curves (ARQ = slope interlobar artery / slope renal cortex).

Results. Thirty-six patients had an uneventful clinical course. In this group US demonstrated a uniform inflow of the USCM with an ARQ of 1.2±0.5 (nonrejection group). Eighteen patients showed histologically confirmed acute rejection on day 5 to 7 after transplantation (rejection group). The ARQ was twice as high in the rejection group (2.3±0.4, $p<0.05$) as in the nonrejection group (1.2±0.5). Eight patients of the nonrejection group with a perirenal hematoma likewise had a higher ARQ (1.5±0.5, $p<0.05$).

C**onclusions.** The use of echo enhancers has a potential for the standardized diagnosis of acute kidney graft rejection. US provides information on the effect of a perirenal hematoma on kidney perfusion.

Physicochemical Properties of Targeted Microbubble Shells

Mark A. Borden

Department of Biomedical Engineering, University of California, Davis 95616

The talk will review some recent experimental results, including theoretical modeling, on the effects composition and structure of the lipid-monolayer shell on its adhesive properties and mechanism of degradation. Examples and comparison of the latter will include static dissolution and destructive insonation. Such studies are revealing new insights and relationships between monolayer structure and lipid shedding behavior. It will be shown and argued that the shell exhibits two phase coexistence, of emulsifier or phospholipid enriched regions, which determines the mechanism of shell collapse and location of targeting ligands and associated nanoparticles. Additionally, a novel brush architecture will be presented that conceals the ligand during transit through non-target areas, thus inhibiting immune recognition and increasing circulation time, but that instantaneously reveals the ligand to achieve targeted adhesion under the influence of ultrasound radiation force. These physicochemical properties will be discussed within the context of applications in ultrasound molecular imaging and drug/gene delivery.

Synthesis, acoustic and optical characterization of monodisperse polymer-shelled ultrasound contrast agents

***Marcel Böhmer*[*#], *Suzanne de Winter*[*], *Jan Steenbakkers*[*], *Christopher Hall*[+], *William Shi*[+], *Annemieke van Wamel*[&], *Marcia Emmer*[&], *Nico de Jong*[&]**

[*]*Philips Research Eindhoven (WAG), Prof Holstlaan 4, 5656 AA Eindhoven, NL*
[+]*Philips Research Briarcliff, 345 Scarborough Road, Briarcliff Manor, NY10510, USA*
[&]*ErasmusMC, Thoraxcentre, Dr. Molewaterplein 50, 3000 DR Rotterdam, NL*

Introduction

Polymer shelled ultrasound contrast agents usually react to the ultrasound field only by release of gas. A number of experimental observations have been made on polymer-shelled agents, which point to size effects and the existence of a threshold acoustic pressure before release of gas can take place (Bouakaz, A.; Versluis, M.; De Jong, N.; *Ultrasound in Medicine and Biology*, **2005**, *31*, 391), Bloch, S. H.; Short, R.E.; Ferrara, K. W.; Wisner, E. R., *Ultrasound in Medicine and Biology*, **2005**, *31*, 439.) Modelling the experimental findings is difficult mainly due to the polydispersity of the agents concerned. In this presentation we will present the synthesis of monodisperse polymer-shelled contrast agents by ink-jet printing, which allows for controlled variations in size and shell thickness. The acoustic properties of these agents are studied using the Brandaris128 fast framing camera and by measuring the acoustic response.

Contrast agent preparation

A solution of the polymer used for the shell and an alkane to form the core in dichloro-ethane (DCE) is inkjetted into an aqueous solution of poly-vinyl alcohol, as schematically depicted in figure 1. This leads to a monodisperse emulsion of liquid droplets in water, that all have the same size. The droplets contain polymer, alkane, and DCE. The DCE slowly diffuses out and evaporates, leading to shrinkage of the emulsion droplets. As the DCE is disappearing the polymer will precipitate and form the shell, while the alkane forms the core of the capsule. After washing, the core is removed by freeze-drying. By tuning the polymer concentration and the alkane concentration the size and shell thickness can be adjusted precisely. A range of particle diameters in between 3 and 9 μm has been prepared with different core to shell ratios.

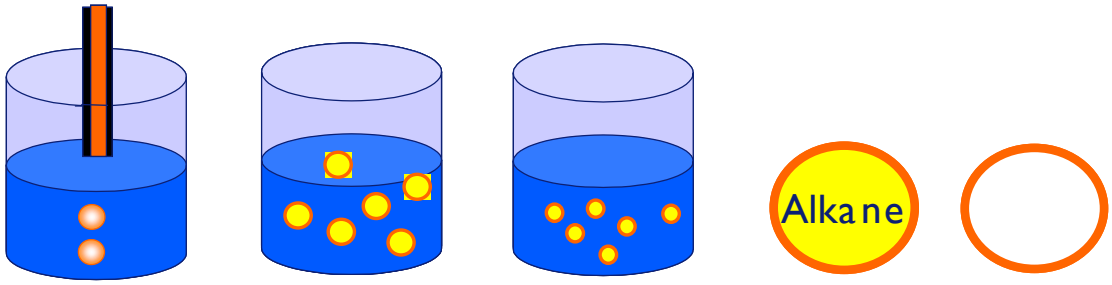

***Figure 1**: inkjetting of a polymer-alkane-dce solution in water and the formation of capsules*

Acoustic Characterization

The acoustic response of single bubbles was determined on very dilute systems with a two-transducer set-up, using a 1 MHz activation transducer and a broadband focused transducer with a centre frequency of 5 MHz for detection. Appropriate filtering techniques were used to eliminate the 1 MHz contribution. The number of acoustic events at a certain acoustic pressure was counted. For all samples a threshold pressure is found, the threshold increasing with decreasing particle size and increasing shell thickness. After the threshold the number of events increases approximately linearly as given in Figure 2.

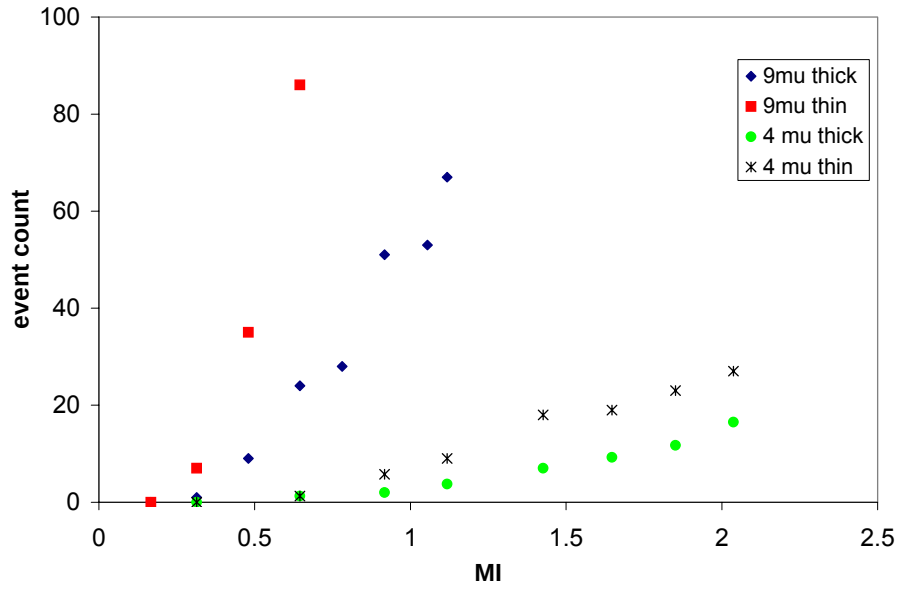

***Figure 2**: Event count for two different particle sizes, each as 2 shell thicknesses*

Optical Observations

None of the capsules showed oscillations. The 9 □m particles were shown to release gas at low acoustic pressure, especially the thin-shelled samples were acoustically very active. The 4 □m particles did not show any release of gas. This agrees with the acoustical data, the 4 □m capsules showed a higher threshold and a lower increase after the threshold had been reached.

Interpretation

The first step in the acoustic activation is the creation of a defect through which gas can escape. Geometric and material properties determine his behaviour. A critical pressure, P_{cr} for a thin-walled spherical pressure vessel can be derived:

$$P_{cr} = \frac{2t\sigma}{r}$$

where *t* is the shell thickness, □is the normal stress and *r* is the radius. This demonstrates the effects of shell thickness and radius as observed experimentally. This analysis will be detailed for a series of sizes and shell thicknesses. After the defect creation gas can escape and the gas bubble formed will interact with ultrasound according to its size.

Acoustical study of the properties of individual phospholipid-based ultrasound contrast agent microbubbles

J. Sijl[1], M. Arditi[2], P.J.A. Frinking[2], N. de Jong[1], D. Lohse[1] and M. Versluis[1]

[1] Physics of Fluids, University of Twente, P.O. Box 217, 7500 AE Enschede, The Netherlands
[2] Bracco Research SA, 31,Route de la Galaise,Plan les Ouates,CH-1228, Genève ,Switzerland

A quantitative study of the acoustic response of a single Ultrasound Contrast Agent (UCA) microbubble at low acoustic pressures is presented.

Objective: Acoustical studies of individual microbubbles require high acoustic pressures, therefore, the dynamic behaviour of these bubbles at low acoustic pressures is generally studied optically. The objective of this study is to look at the acoustic response of individual microbubbles insonified at low acoustic pressures.

Materials and methods: Our setup consists of a transmit transducer transmitting a pulsed ultrasound beam, exiting a single bubble confined in a 200 μm capillary tube positioned at the focal point of the transducer. A second receive transducer, focussed at the same point, is used to collect the echo coming from the individual bubble. Both transducers and the capillary tube were made to fit onto the translation stage of an inverted microscope. Simultaneous optical observations were analyzed to determine the resting radius of the bubble and to ensure that a single bubble was present within the ultrasound beam. The complete acoustic setup was calibrated, both on transmit and receive. The calibration procedure included beam diffraction as well as the impulse response of the receiving transducer. In this way, the UCA bubble response was studied in an absolute and quantitative way. Individual echo waveforms were analyzed by a best-fit analysis with a parametric bubble model [1]. The acoustical responses of a total of 109 microbubbles with sizes ranging from one to five micrometer (radius), subjected to a five-cycle 2 MHz sinusoidal acoustic pulse with a peak rarefactional amplitude of 60 or 120 kPa, were recorded.

Results: With this setup we were able to measure the acoustic responses of single bubbles with a radius as small as 1 μm. Furthermore, based on the fit between the experimentally obtained acoustical responses and the parametric bubble model model [1], the viscoelastic parameters of lipid-shell microbubbles are determined.

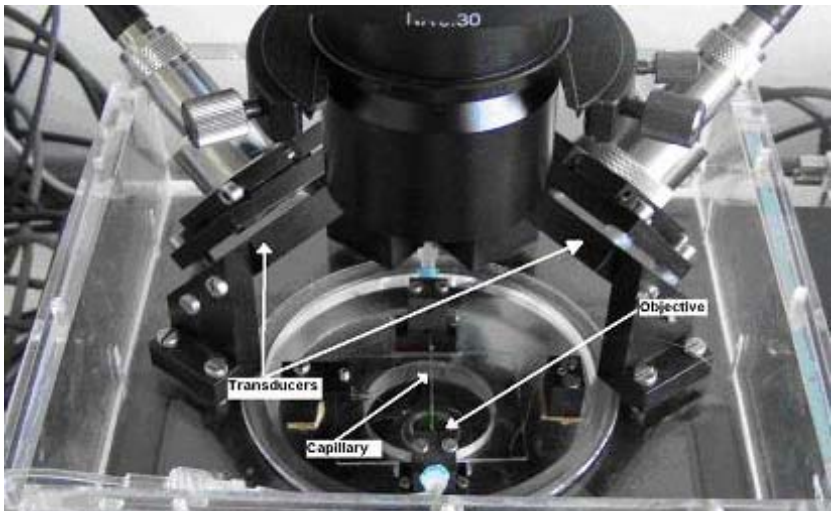

Figure 1*: The experimental setup. This system allows for simultaneous acoustical and optical observations of single microbubbles guided through a small cellulose capillary tube.*

[1] Marmottant, P., van der Meer, S., Emmer, M., Versluis, M., de Jong, N., Hilgenfeldt, S., Lohse, D., "A model for large amplitude oscillations of coated bubbles accounting for buckling and rupture", J. Acoust. Soc. Am. 118 (6), December 2005

Experimental Observation of Cell Membrane Rupture by Microbubble Cavitation

Paul Prentice & Paul Campbell.

Institute of Medical Science & Technology, Department of Surgery and Molecular Oncology, Ninewells Hospital, University of Dundee, Dundee DD1 9SY. Scotland, UK

Enhanced permeabilisation of cells via insonation in the presence of ultrasound contrast agent (UCA) has been recognised for well over a decade. Development of the approach for drug delivery within a clinical context has been inhibited by a lack of understanding of the ultra-fast UCA-membrane interactions. Here, we have developed an innovative apparatus utilising holographic optical trapping to achieve spatial control of UCA, which affords a level of experimental flexibility hitherto unseen in this context. Insonation of isolated microbubble-cell configurations with parallel high speed microphotography, and downstream inspection via atomic force microscopy, has allowed us to identify several distinct permeabilization modes. **(*viz* Nature Physics, 1, (2) 107 (2005))**

The fundamental mechanism of interaction between cell and microbubble during insonation remains elusive and this has hampered attempts to optimise the approach. In addressing this deficiency in our understanding, we designed and constructed a unique apparatus that can optically guide an individual UCA microbubble to a predefined displacement relative to a planar substrate. In parallel with this, we undertook direct observations, via high speed imaging at MHz frame rates. We demonstrate how this approach has allowed us to observe a dynamic microscopic interaction during insonation, that gives rise to membrane permeabilization in biological cells. We show directly that ultrasound activated UCA in proximity to rigid boundaries can undergo microjet formation directed towards the surface. The consequences of this occurrence, if transposed into a biomedical context may go some way to explaining the mechanism whereby cells are permeabilised via insonation in the presence of UCA.The hybrid trapping/insonation apparatus uses a refined holographic Laguerre-Gauss optical trap to maintain a single low index UCA at a controlled distance above a substrate. With the high speed camera synchronised to acquire data upon triggering via a TTL pulse (that also initiates the US burst) data can then be obtained with the required spatial and temporal resolutions. In the first instance we attempted to observe the dynamic behaviour of individual UCA at controlled proximities to naked coverslip substrates. By trapping the UCA microbubble typically to within five bubble diameters of the substrate, we were able to observe cavitation. Occasionally we noticed the formation of a micro-jet structure that involutes to traverse the entire bubble (figure below). The initial stage appears to involve involution at the furthermost pole from the substrate followed by the emergence of a jet directed at the substrate.

The sequence illustrated below used a 5μm microbubble insonated at a peak negative pressure of 0.6MPa as a 20μs burst. Our presentation will also show other examples ultrasound activated microbubbles that may also rupture the cell membrane and indicate their statistical significance.

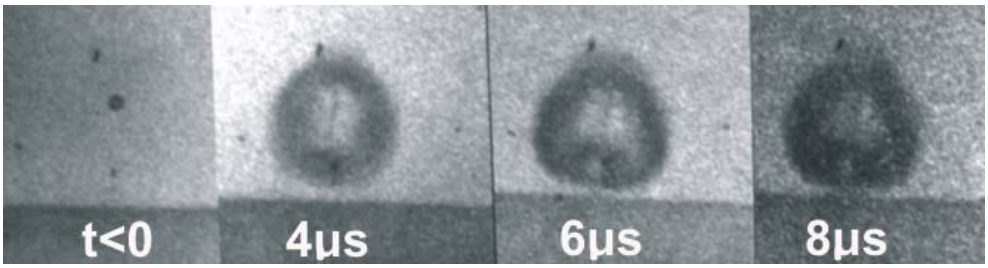

Microjet formation in optically trapped Optison. The jet 'touches down' in frame 4

A New Ultrasound Imaging Method for Molecular Imaging

Jim Chomas, PhD

Siemens – Mountain View CA – USA

The health care continuum for medical imaging encompasses prediction, diagnosis, treatment and follow-up. Currently, ultrasound is extensively involved in diagnosis. Molecular Imaging allows the expansion of ultrasound to prediction and treatment. Prediction can be achieved with ultrasound through the use of targeted agent imaging and screening, and the inclusion of multiple modalities into an integrated set of clinical information. Treatment can be achieved with clinical diagnostic ultrasound with the use of imaging agents.

Prediction and screening require excellent imaging sensitivity as well as highly streamlined workflow. A new imaging mode, called Convergent CPS (Contrast Pulse Sequencing), combines the excellent sensitivity and specificity with unique information on the agent, such as the velocity and relative frequency response. CNV allows imaging of targeted agents immediately following injection, greatly improving the workflow in terms of time and processing complexity. The CNV imaging method is also extended to pulsed-wave applications for optimized agent specificity, offering improved quantification of flow dynamics during an agent study. Results of PW CNV are shown in Figure 1, in a study of the LAD in a dog model. In Figure 1a, the standard PW imaging shows significant artifacts from tissue motion, affecting the quality of the PW shape. In Figure 1b, PW CNV shows only information from agents moving in the LAD and tissue motion information is filtered out.

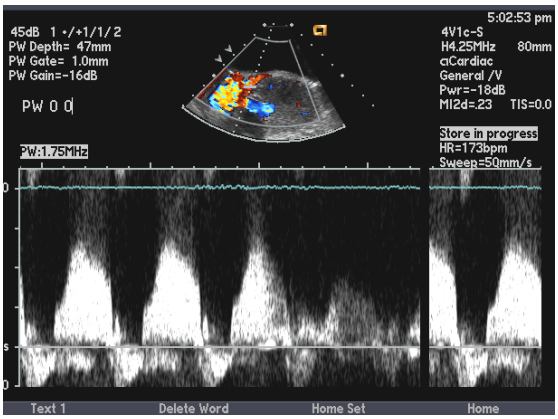

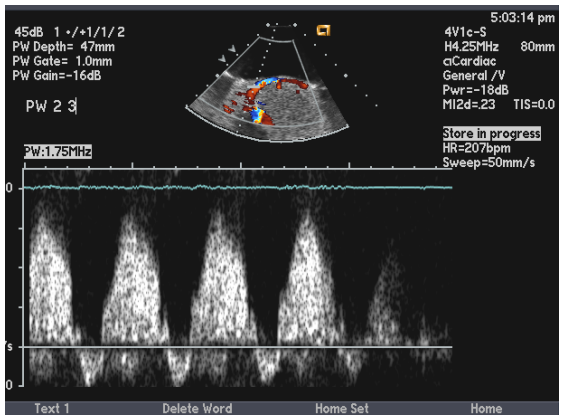

Treatment applications, ranging from stroke to coronary stenosis to deep vein thrombosis, require methods that combine high resolution imaging combined with optimized therapeutic transmit pulses. With the use of new agents that are targeted and or loaded with a thrombolytic agent, treatment with diagnostic ultrasound is possible. Early animal studies suggest the combination of CPS agent imaging with new therapeutic pulses provides rapid clot dissolution in newly formed clots.

Siemens is developing Ultrasound Molecular Medicine to expand applications toward early prediction and treatment. Cadence CPS Ultrasound is well suited for Molecular Imaging compared to other imaging modalities due to real-time image acquisition, low toxicity, ability to affect agent clearance time, and ability to perform treatment.

Imaging Angiogenesis

Peter N. Burns

Depts Medical Biophysics and Radiology - University of Toronto, Canada

Of those areas of diagnostic application emerging for contrast ultrasound, one of the most intriguing is the challenge of imaging *angiogenesis*. Angiogenesis is the term used to describe the development of a microscopic blood supply to tissue. It occurs during normal embryonic vascular development and organogenesis as well as such physiological processes as wound healing and the female menstrual cycle. Angiogenesis of the *vasa vasorum* is known to occur in atherosclerosis, though its precise significance is not known. It is well understood, however, to be a key element of the development of a cancer, providing the blood supply to a tumour which subsequently allows its malignant progression [1-3]. Without such a supply, a breast cancer *in situ*, for example, will grow to a few millimetres and remain harmless. It is estimated that about 40% of women aged 40-50 have such lesions, yet less than 1% go on to have clinical cancer [4]. This minority of lesions undergoes a process known as *malignant angiogenesis*, in which new vessels grow from the host into the cancer. The vessels provide a supply of oxygen and nutrients for the cancer cells to grow, as well as a conduit through which they can metastasize to distant organs in the body. From a diagnostic point of view, it these angiogenic lesions, not every breast lesion, that we need to be able to identify; hence the importance of being able to image angiogenic vessels. Therapeutically, the deliberate induction of angiogenesis in ischemic tissue such as infracted myocardium has also become one of the objectives of molecular therapies for regeneration. Advances in the understanding of angiogenic transformation, and particularly the potential to modulate it using new drugs, have propelled this field into the forefront of cancer research [5]. Angiogenesis in breast cancer, for example, has implications for diagnosis, prognosis and treatment. Identifying those breast cancers which have new blood vessels may help to distinguish ductal carcinomas *in situ* from the much smaller number among them which are exhibiting malignant progression and presumably need to be treated more aggressively. Once a cancer has been identified, it is been shown that the number and density of blood vessels provides additional prognostic information which is independent of clinical staging, perhaps offering potential to better tailor therapy to an individual patient's disease. Finally, a large number of new treatment strategies target the proliferating vasculature of a developing cancer, including drugs specifically designed to inhibit the angiogenic transformation itself. For these reasons, the ability to provide imaging information on the status of blood supply to breast cancer is of enormous clinical significance.

Direct imaging of the angiogenic circulation is extremely challenging, as the vessels are small, pathological and beyond the resolution limit of conventional radiological imaging [6]. However, their pathological characteristics, which influence both morphology and the dynamic properties of blood flowing within them, offer several possibilities for identification by noninvasive means. Magnetic resonance imaging, for example, appears to be capable of revealing the presence of these vessels by virtue of their increased permeability. Contrast ultrasound imaging may be able to show changes in the volume of tumour tissue occupied by blood, as well as changes in overall flow rate at the microvascular level. It has the advantage over other modalities of providing real-time imaging, a true blood pool agent (the malignant neovasculature is hyperpermeable and hence CT and MR agents leak into the interstitium), and the ability to detect individual bubbles flowing in capillary vessels. But measuring properties of the angiogenic vasaculature is not simple. The conventional disruption-replenishment model, has been shown to be dependent on vascular morphology, and account has yet to be made of the chaotic and dysmorphic malignant vasculature, which will affect both flow and volume estimates [7]. These are certainly important to assess the response to ablative and antivascular therapies. For diagnosis, however, many cancers have a similar bulk flow rate and volume as normal tissue. What is needed is some indication of the *morphological* changes to the vasculature brought about by malignant transformation. Although the angiogenic vessels lie below the resolution of the ultrasound image, the ability to detect individual bubbles is exploited further in a method where individual bubbles are tracked as they pass through the tumour, building an image reflecting morphological structure in the tumour. Dramatic differences are evident between benign hyperplastic lesions, such fibroadenoma and focal nodular hyperplasia, and cancers.

This combination of hemodynamic and morphological methods is being applied successfully to the quantitative monitoring of anti-angiogenic therapies in animal models, and is now beginning to be applied in the significant number of clinical trials of new anti-angiogenic agents awaiting assessment [8]. Some preliminary results from the anti-vascular tubulin-rounding agent ZD6126 will be shown [9]. If the low toxicity and host resistance to such drugs is coupled with their dramatic impact on the growth of cancer, as has been demonstrated clinically with the first FDA-approved anti-angionic agent Avastin [10], it is likely that the unique ability of contrast microbubbles to measure angiogenic blood flow in an quantitative and inexpensive manner will create a new and exciting area of application for ultrasound contrast imaging.

References

1. Folkman J, Merler E, Abernathy C, Williams G. Isolation of a tumor factor responsible or angiogenesis. J Exp Med 1971; 133:275-88.
2. Hanahan D, Folkman J. Patterns and emerging mechanisms of the angiogenic switch during tumorigenesis. Cell 1996; 86:353-64.
3. Folkman J. Incipient angiogenesis. Journal of the National Cancer Institute 2000; 92:94-5.
4. Black WC, Welch HG. Advances in Diagnostic Imaging and Overestimations of Disease Prevalence and the Benefits of Therapy. New England J Med 1993; 328:1237-43.
5. Kerbel R, Folkman J. Clinical translation of angiogenesis inhibitors. Nature Reviews Cancer 2002; 2:727-39.
6. McDonald DM, Choyke PL. Imaging of angiogenesis: from microscope to clinic. Nature Medicine 2003; 9:713-25.
7. Karshafian R, Burns PN, Henkelman MR. Transit time kinetics in ordered and disordered vascular trees. Phys Med Biol 2003; 48:3225-37.
8. Foster FS, Burns PN, Hope Simpson D, Wilson SR, Christopher DA, Goertz DE. Ultrasound for the visualization and quantification of tumor microcirculation. Cancer and Metastasis Reviews 2000; 19:131-8.
9. Goertz DE, Yu J, Kerbel RS, Burns PN, Foster FS. High frequency Doppler ultrasound monitors the effects of antivascular therapry on tumor blood flow. Cancer Research 2002; 62:6371-5.
10. Preda A, Novikov V, Moglich M, et al. MRI monitoring of Avastin antiangiogenesis therapy using B22956/1, a new blood pool contrast agent, in an experimental model of human cancer. J Magn Reson Imaging 2004; 20:865-73.

Imaging of Prostate using Contrast

Ferdinand Frauscher

Department of Radiology II, Medical University Innsbruck, Austria

Background: The annual incidence of prostate cancer has increased dramatically over the past decade such that prostate cancer is now the most commonly diagnosed visceral malignancy in men. Prostate specific antigen (PSA), digital rectal examination (DRE) and ultrasound (US) guided biopsy are the routinely used diagnostic tests, which however lack both sensitivity and specificity.

Methods: We have used US contrast agents for colour and power Doppler US, and grey scale harmonic imaging in patients with elevated PSA and/or abnormal DRE. Gray scale harmonic imaging was performed in continuous and intermittent mode. Furthermore the US contrast administration was done either with bolus or infusion technique. Time intensity curves were assessed after US contrast injection. Prostate cancer detection rates were compared with systematic biopsy findings or histopathology obtained after radical prostatectomy.

Results: 537 of 1540 patients (35%) had prostate cancer with a mean PSA of 3.9 ng/mL. Prostate cancer was detected by contrast enhanced targeted biopsy in 447 patients (29%), and in 339 patients (22%) with systematic biopsy. Out of 7225 targeted cores 997 (13.8%) were positive, and 800 out of 15400 systematic cores (5.2%). The cancer detection rate was significantly improved by using contrast-enhanced targeted biopsy ($p<0.01$). Intermittent imaging was found to improve cancer detection when compared with continuous imaging. The transit time analysis showed an earlier and higher enhancement and a faster wash-out in cancer tissue when compared with normal prostatic tissue.

Conclusion: Contrast-enhanced US has shown to improve prostate cancer detection when compared with systematic biopsy. Assessment of time intensity curves, the use of intermittent imaging and administration of contrast in an infusion technique seems further to improve the differentiation between benign and malignant prostatic tissue. However, future clinical trials will be needed to determine if the promise of contrast US of the prostate evolves into clinical application.

New developments in therapeutic applications of microbubbles

Raffi Bekeredjian

Dept. of Cardiology, University of Heidelberg, Germany

Gas filled microbubbles have become an important tool in diagnostic ultrasound as contrast agents to enhance image quality and characterize myocardial perfusion. Their physical properties allow both visualization by low mechanical index ultrasound and destruction of microbubbles by high mechanical index ultrasound. Ultrasound targeted microbubble destruction has lead to the development of a new therapeutic application. Microbubbles loaded with a bioactive substance can be destroyed in a target organ or tissue, thus allowing for non-invasive delivery of drugs or gene therapy vectors, such as virus or plasmid DNA. In addition, microbubble destruction per se may have advantageous local effects that can be used for thrombolysis and stimulation of arteriogenesis.

Most applications of therapeutic ultrasound targeted microbubble destruction have been tested in cardiac models. One of the main aims was to develop new strategies for gene therapy. More recently, this field has been extended to other ultrasound accessible organs for drug and gene delivery. Skeletal muscle, blood vessels, kidney, pancreas and central nerve system are among successfully tested targets. Here again, gene delivery is the main therapeutic aim. However, drug delivery may play an important role in future applications of this technique, trying to minimize side effects in tumor therapy or to overcome pharmacologic sanctuaries, such as the blood-brain or blood-testis-barrier. New microbubble formulations and refined ultrasound machines could improve the efficiency of this technique.

Ultrasound contrast agent mediated temporal adjusted vascular permeability

Annemieke van Wamel [1-2]***, Klazina Kooiman*** [1] ***, Folkert ten Cate*** [3] ***and Nico de Jong*** [1-2-4]

1-Dept. of Biomedical Engineering, Thoraxcentre, Erasmus MC, Rotterdam, The Netherlands
2-ICIN, Utrecht, The Netherlands
3- Dept. of Cardiology, Thoraxcentre, Erasmus MC, Rotterdam, The Netherlands
4- Dept. of Applied Physics, Physics of Fluids, University of Twente, Enschede, The Netherlands

Background: Circulating blood provides oxygen, nutrients and hormones to the tissues and removes carbon dioxide and waste products. The exchange of these factors is regulated by the endothelium, which forms the interface between blood and tissues. The endothelium controls the extravasation of solutes, macromolecules and white blood cells, and maintains a continued flow of blood by preventing loss of blood constituents and volume. Sometimes, a controlled, temporal, and local increase in endothelium permeability can be desired, for example, with the aim to enhance drug delivery.

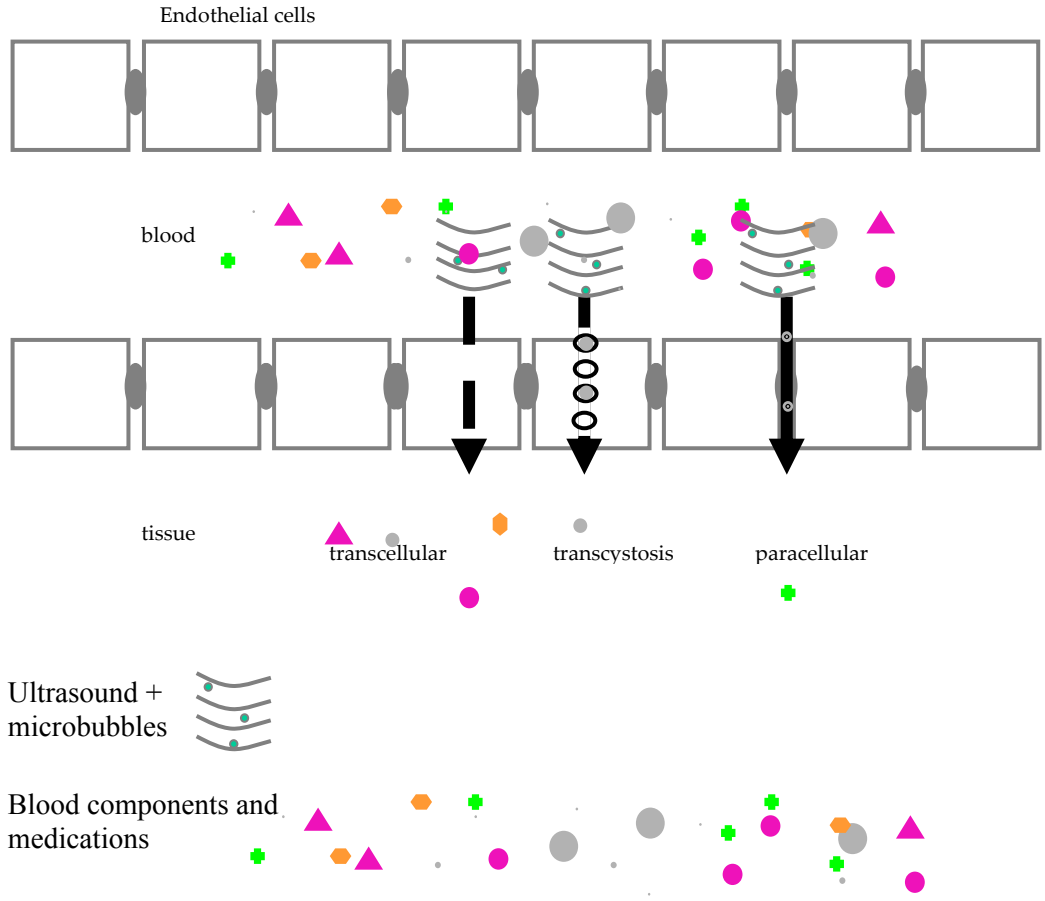

Figure 1. *Scheme temporal ultrasound contrast mediated locally hyperpermeable endothelium*

Current therapeutic contrast research*:* Vessel leakage can be induced by creating gaps between endothelial cells as well as by the induction of transcellular transport pathways. Here, the mechanisms that may be involved in the ultrasound microbubble controlled vascular permeability are being discussed. We focus on the dynamic interactions between the endothelial cell-layer and ultrasound activated microbubbles. Due to forces generated by oscillating microbubbles, the endothelium becomes locally hyperpermeable, allowing transendothelium flux of fluid and macromolecules for during a short period of time via mechanical mechanisms including pore formation (trans cellular) and biological mechanisms like vesicle formation (trans cystosis) (fig 1).

Therapeutic opportunities*:* In principle, ultrasound controlled microbubble mediated drug delivery could play a pivotal role in altering the biodistribution and pharmacokinetic profile of several drugs to yield a better efficacy and safety profile. Delivering therapeutic agents to specific molecular targets in the cardiovascular tissues is not a simple task. There are still many questions yet to be answered like how efficient can an endothelium layer be permeabilized? Since the endothelium structure and fenestration of vessels are heterogeneous in tissues, will macromolecular therapeutics be delivered more selectively to the vessel wall than low molecular weight drugs? These questions have to be addressed in a rational manner.

Myocardial contrast enhancement with real-time time imaging allows accurate assessment of myocardial perfusion and improves the diagnostic value of standard stress echocardiography

P Lipiec[1], P Wejner - Mik[1], M Krzeminska - Pakula[1], L Chrzanowski[1], M Plewka[1], J Drozdz[1], J Kusmierek[2], A Płachcinska[2], R Szuminski[2], JD. Kasprzak[1]

[1] II Chair and Department of Cardiology, Medical University of Lodz, Lodz, Poland
[2] Department of Nuclear Medicine, Medical University of Lodz, Lodz, Poland

Background: Gated 99mTc-sestamibi SPECT (G-SPECT) is considered one of the reference methods for assessment of myocardial perfusion. The diagnostic value of stress echocardiography based on evaluation of wall motion abnormalities (WMA) has also been extensively studied. However, the diagnostic potential of stress real-time myocardial contrast echocardiography (MCE) has not been fully established.

Aim: To assess the diagnostic value of stress real-time MCE for detecting perfusion defects in comparison with G-SPECT and to assess if MCE improves the diagnostic accuracy of standard stress echocardiography in patients with suspected stable coronary artery disease (CAD).

Methods: 55 patients (pts) (35 male, mean age 57±9 years) with suspected stable CAD (mean CCS class 2,5) scheduled for coronary angiography were included in this prospective study. 29 pts had no history of myocardial infarction (MI). Prior to coronary angiography all pts underwent G-SPECT and high-dose dipyridamole (0,84mg/kg iv over 4 minutes)-atropine (up to 1mg iv) stress real-time MCE (Contrast Pulse Sequencing, Siemens Sequoia C256) using repeated iv boluses of Optison and visual scoring of WMA and perfusion in 18 segments of left ventricle. Presence of significant CAD (>=70% stenosis or >=50% stenosis of left main coronary artery) was detected by coronary angiography.

Results: Assessment of MCE was feasible in 96% of segments at rest and 94% at peak stress. Agreement between G-SPECT and MCE was 84% in detecting any (inducible or fixed) perfusion defects and 66% in detecting inducible defects. In a subgroup of pts with no history of MI the agreement was 72% in detecting any perfusion defects and 66% in detecting inducible defects. Significant CAD was present in 75% of pts (33%-1 vessel, 25%-2 vessels, 16%-3 vessels). Presence of inducible WMA had 67% accuracy (59% sensitivity, Se; 86% specificity, Sp) in detecting significant CAD. Concomitant assessment of MCE provided 84% accuracy (85% Se; 79% Sp) using presence of any inducible abnormality (WMA or perfusion defects) as a criterion.

Presence of inducible perfusion defects detected by G-SPECT had 62% accuracy (71% Se; 36% Sp). Presence of any (inducible or fixed) WMA had 85% accuracy (93% Se; 64% Sp), whereas presence of any perfusion defects in G-SPECT had 80% accuracy (95% Se; 36% Sp). However, the optimal diagnostic accuracy was achieved using the following echocardiographic criterion: any inducible or fixed WMA or perfusion defect – 87% (98% Se, 57% Sp). In a subgroup with no history of MI presence of any perfusion defects in G-SPECT had 66% accuracy (88% Se; 39% Sp), whereas MCE provided 79% accuracy (94% Se; 62% Sp) using the criterion of any WMA or perfusion defect.

Conclusions: Stress real-time MCE offers acceptable agreement with G-SPECT in detecting myocardial perfusion defects. Similar sensitivity and higher specificity result in higher accuracy of MCE compared to G-SPECT. Moreover, MCE improves the diagnostic accuracy of standard stress echocardiography.

Study supported from KBN grant P05B 03623.

Contrast Intravascular Ultrasound: Progress Towards Coronary Artery Vasa Vasorum Imaging

DE Goertz[1,2], ME Frijlink[1], D Tempel[1], LCA van Damme[1], R Krams[1,2], JA Schaar[1,2], FJ ten Cate[1], N de Jong[1,2,3], AFW van der Steen[1,2]

1- Erasmus MC, Rotterdam the Netherlands, 2- Interuniversity Cardiology Institute of the Netherlands, 3- Physics of Fluids, Twente University

It is increasingly recognized that the development of neovascular vasa vasorum is necessary for atherosclerotic plaque progression and may promote lesion instability. At present, there are no clinical tools capable of performing high resolution imaging of coronary artery vasa vasorum, which may provide information relevant to the identification of vulnerable plaques. The objective of the present research is to develop and investigate intravascular ultrasound (IVUS) contrast agent techniques for assessing the microvascular status of atherosclerotic plaques. One strategy being pursued is to examine image enhancement following the injection of modified commercial agents. A second strategy is to employ targeted microbubbles.

Methods

Instrumentation:

A prototype nonlinear IVUS system was developed for tissue harmonic and contrast agent imaging. The approaches discussed in this presentation will be second harmonic imaging of a 20 MHz transmit pulse and subharmonic imaging of a 40 MHz transmit pulse. The detection of these signals was facilitated by the use of specialized single element mechanically scanned IVUS transducers developed to have a frequency response with peaks at 20 and 40 MHz.

Contrast Agents:

For free microbubble experiments, commercially available agents were modified through decantation procedures to produce relative improvements in high frequency acoustic activity. Attenuation was measured over the 2 to 50 MHz range in native and decanted Definity populations. A 15 minute in-vial decantation time, for example, resulted in a loss of 42% of the microbubble volume fraction, and produced attenuation that peaked in the 10 to 30 MHz range.

For targeted microbubble experiments, we employed an experimental biotinated micron sized lipid encapsulated agent (BG3039, Bracco Research).

Imaging Experiments:

In vivo studies were conducted in atherosclerotic rabbit aortas. The IVUS catheter was situated in a region of interest in the aorta and agent was released proximally in the form of a bolus through a delivery catheter. Imaging data was acquired for 60 seconds following injection to examine the bolus dynamics. Tissue was then excised for histology, which was conducted with both H/E and CD31 endothelial cell staining.

In vitro targeting experiments were conducted by binding the biotinated microbubbles to an avidin coated agar phantom.

Results

For the in vivo second harmonic imaging experiments, agent was first detected within the main lumen, followed by its presence in adventitial microvessels. The general spatial pattern of enhancement was consistent with that observed in the histologic sections. A quantification of adventitial enhancement following injection was found to be statistically significant. These results suggest the potential for contrast IVUS as a technique for imaging vasa vasorum.

The targeted bubble experiments demonstrated that nonlinear emissions were possible to stimulate from bound microbubbles. Both second harmonic and subharmonic imaging modes were found to improve the contrast to tissue ratio relative to fundamental frequency imaging. These results indicate the potential of nonlinear targeted microbubble imaging techniques may be an alternative strategy for IVUS vasa vasorum imaging.

Acknowledgements: This work was financially supported by the Dutch Technology Foundation (STW). Definity™ was provided by Bristol-Myers Squibb, and BG3039 by Bracco Research (Geneva).

Measuring Neovacularization Using Contrast Enhanced Carotid Artery Ultrasound — A New Surrogate Marker of Atherosclerosis

Falak Shah B.S., Prakash Balan, M.D., Matthew Weinberg, M.D., Vijaya Reddy, M.D., Marshall Goldin, M.D., Steven B. Feinstein, M.D.

Rush University Medical Center, Chicago, Illinois, USA

Objectives: The present study seeks to demonstrate that contrast enhanced carotid artery ultrasound (CE-CU) constitutes an effective method for the early detection of atherosclerotic disease.

Background: Atherosclerotic plaques are sustained by the neovascularization of vasa vasorum on the adventitial surface of blood vessels. Such neovascularization develops very early in the pathogenesis of atherosclerotic plaques. Contrast enhanced carotid artery ultrasound (CE-CU) is capable of imaging this neovascularization and thus allows for the early detection and treatment of systemic atherosclerotic disease.

Methods: Eighteen patients found to have carotid artery disease underwent contrast enhanced carotid artery ultrasound (CE-CU) prior to undergoing carotid endarterectomy. Plaque samples taken during endarterectomy were stained with the following markers of vascularity: CD31, CD34, Factor VIII, and hemosiderin. The grading of neovascularization obtained from pre-operative CE-CU was then correlated with the grading of neovascularization obtained from the surgical specimens stained with the above mentioned vascular markers.

Results: Comparison of the CE-CU assessment of vascularity with the histopathologic assessment of vascularity, employing CD31 as the marker of vascularity, revealed a correlation of 0.68. Similarly, comparison of the CE-CU assessment of vascularity with the average histopathologic assessments of four separate vascular markers (CD31, CD34, Factor VIII, and hemosiderin) revealed a correlation of 0.505.

Conclusions: CE-CU therefore effectively detects the neovascularization associated with atherosclerotic disease and thus CE-CU serves as an effective method of detecting systemic atherosclerotic disease.

Molecular Imaging of Angiogenesis

Jonathan R. Lindner, MD

University of Virginia Medical Center, Charlottesville, Virginia, USA

It has recently become possible to target microbubble contrast agents to disease-related cellular and molecular processes. Targeting has been possible by either changing the chemical constituents on the bubble shell, or by conjugating specific ligands to the surface of the microbubbles. Our lab has successful at imaging both inflammatory processes and angiogenesis by targeting endothelial cell adhesion molecules. In this talk we will discuss some recent advances in each of these fields and how they relate to improving therapy.

Microbubbles targeted to angiogenesis have been developed by conjugating the disintegrin echistatin, which binds to alpha-v beta-2 integrins, to the surface of lipid-shelled microbubbles. This agent has been shown to adhere to neovessels in matrigel models of angiogenesis and in glioblastomas in rats. We have recently used this agent in a rat hind-limb model of angiogenesis to image endogenous and therapeutic angiogenesis. Occlusion of the iliac artery in rats resulted in a reduction of resting flow, measured by MCE, to approximately one third of normal. The endogenous angiogenic response resulted in an increase in blood flow to just over half of normal by 14-28 days. This increase in blood flow was preceded by a peak in the signal from angiogenesis-targeted microbubbles at day 4-7, which was also the peak of alpha-v integrin expression on immunohistochemistry. In rats treated with slow-release FGF-2 after iliac occlusion, perfusion increased faster and to a greater degree than non-treated rats (reaching 75% of normal). In FGF-2-treated compared to non-treated rats, the signal from angiogenesis-targeted microbubbles at 4-7 days was greater. These data demonstrate that alpha-v beta-3-targeted microbubbles can provide data on the extent of endogenous and therapeutic angiogenic responses prior to any measurable changes in blood flow.

We have previously used microbubbles targeted to endothelial cell adhesion molecules and to leukocytes to study inflammatory responses to ischemia-reperfusion injury in the heart and kidney. More recently, we have developed microbubbles targeted to MAdCAM-1, which is selective for gastrointestinal inflammation, in order to diagnose and follow inflammatory bowel disease. Flow chamber studies have demonstrated selective adhesion of these targeted microbubbles to stimulated cells that express MAdCAM-1. Contrast imaging with MAdCAM-1-targeted microbubbles in SAMP1/YitFC mice which develop spontaneous Crohn's disease has demonstrated intense bowel and medial lymph node enhancement.

Enhancement was very low for non-targeted microbubbles in these animals and for targeted microbubbles in control mice (AKR). These data demonstrate that assessment of inflammatory bowel disease may be possible with ultrasound and microbubbles targeted to MAdCAM-1. This method may be valuable in the clinical setting for early diagnosis and for differentiating disease flares from chronic changes, for which there is no diagnostic technique currently available.

Finally, gene delivery and drug delivery are possible with custom microbubble carriers. There is now evidence that tissue deposition of these therapeutic agents is more efficient when microbubbles are apposed or in proximity to the vessel wall, which can be accomplished with targeting.

Highly-Targeted Retroviral Gene Delivery Using Ultrasound

Sarah L. Taylor[1], Ahad Rahim[1], Nigel Bush[2], Jeffrey C. Bamber[2] & Colin D. Porter[1]

The Institute of Cancer Research, [1]Section of Cell and Molecular Biology, 237 Fulham Rd., London SW3 6JB [2] Joint Department of Physics, The Institute of Cancer Research and The Royal Marsden NHS Trust, Downs Road, Sutton, SM2 5PT UK

Gene therapy for the treatment of chronic and acute diseases would be improved with the development of a vector that achieves site-specific, long-term gene expression. Retroviral integration results in permanent gene expression; however, specificity of delivery represents the major problem limiting clinical application of retroviral vectors. We have addressed this problem by developing a novel retroviral delivery methodology. *In vitro*, ultrasound-targeted gene delivery to a pre-determined area of cells was achieved using cationic microbubbles loaded with infection-deficient murine leukemia virus particles. Gene delivery efficiencies of up to 2% were achieved near the beam focus, where ultrasound peak negative pressures of 0.5-1MPa were measured. The significant transduction achieved was restricted to areas exposed to $\geq$0.5MPa acoustic pressure despite uniform application of the MLV vector to all cells. This demonstrated an ultrasound pressure threshold that can be exploited for targeted retroviral transduction. The methodology readily lends itself to implementation for controlling retroviral gene delivery *in vivo* following systemic administration.

The novelty of our approach is that spatial control at a distance is exerted upon viral delivery by subsequent exposure to ultrasound. For eventual clinical application, this process is non-invasive and the necessary acoustic pressures can be applied specifically to the target site. Our data provide a solution to the critical issue of tissue specificity following systemic administration of retroviral vectors.

Contrast enhanced B flow imaging for the evaluation of periadventitial vasa vasorum in human carotid atherosclerosis

Magnoni M, Coli S, Melisurgo G, Cianflone D, De Dominicis D, Marrocco-Trischitta MM, Chiesa R, Feinstein SB,* Maseri A.

*Dep. of Cardiothoracic and Vascular diseases, Vita-Salute University, San Raffaele Scientific Institute, Milan , Italy; *Rush University Medical Center, Chicago, USA*

Background Recent studies in the animal model have found an important role of arterial vasa vasorum during the atherosclerotic process. In particular, Kwon et al have demonstrated an increase in the network of periadvential vasa vasorum by micro CT after hypercholesterolemic diet. High cholesterol diet produced intima-media thickening and a relative hypoxic status of the media layer, that could induce the proliferation of adventitial vasa vasorum to improve nutrition supply.
The aim of the present study was to explore the possibility that ultrasound imaging with contrast agent is able to visualize adventitial vasa vasorum in human carotid atherosclerosis.

Methods We studied 25 patients with carotid stenosis > 50% (ATS group) and 15 patients without any carotid artery plaque and an intima-media thickness (IMT) less than 1.0 mm (CTRL group). The two groups were matched for age, sex and risk factors (including arterial hypertension, hypercholesterolemia, active smoking and diabetes mellitus).
In all patients carotid arteries were studied with a Vivid 7 (GE-Healthcare) ultrasound machine using 7 L probe. Standard B mode, color Doppler and PW Doppler were performed to evaluate the presence of plaques and the degree of stenosis. Far wall IMT was measured bilaterally at the level of the common carotid artery. To study periadventitial vasa vasorum we used intravenous injection of Optison (GE-Healthcare), a pure vascular ultrasound contrast agent composed by perflutren and albumin, and a low MI setting (0.08-0.10). B-flow imaging modality was used to improve periadventitial flow signal: after background subtraction the thickness of the linear adventitial flow signal was measured in the far wall of the common carotid artery.

Results on contrast enhanced images a fast microbubble flow was detectable in the adventitial area in all patients of both groups. Also, all patients presented a homogeneous and linear periadventitial contrast signal using B-flow imaging.
As expected from the inclusion criteria, IMT was higher in ATS group than in CTRL group (mean $\pm$ SD: CTRL 0.73 $\pm$ 0.13 mm; ATS 1.08 $\pm$ 0.14 mm; $p< 0.001$).

Periadventitial signal thickness by B-flow imaging was higher in patients with atherosclerosis than in the control group (median, 25°-75° percentile: CTRL 0.8, 0.75-0.8 mm; ATS 1.1, 1.01-1.2 mm; $p < 0.0001$). Moreover, considering the whole study population of 40 patients, the thickness of the adventitial signal presented a linear relation with IMT values (r^2 0.77 $p < 0.0001$).

Conclusions In our study all patients presented periadventitial contrast flow signal. Patient with carotid atherosclerosis had a higher periadventitial contrast signal thickness by B-flow imaging than control patients. This finding is consistent with animal studies showing adventitial vasa vasorum proliferation early in the atherosclerotic process. The periadventitial contrast signal thickness by B-flow imaging is correlated with intima-media thickness. According to our results ultrasound imaging with contrast agent is useful to detect and to evaluate periadventitial vasa vasorum in human carotid arteries.

Bubbles for therapy: manipulation of endothelial layer permeability

Klazina Kooiman[1], Miranda Harteveld[1], Nico de Jong[1-2-3] and Annemieke van Wamel[1-2]

1- Dept. of Biomedical Engineering, Thoraxcentre, Erasmus MC, Rotterdam, The Netherlands
2- Interuniversity Cardiology Institute of the Netherlands, Utrecht, The Netherlands
3- Dept. of Applied Physics, Physics of Fluids, University of Twente, Enschede, The Netherlands

Background: For many drugs crossing the endothelial barrier is very difficult. An increase in permeability may have important clinical implications, as a more efficient delivery of drug to the damaged tissue would be expected. In this study ultrasound contrast agent enhanced endothelial layer permeability is studied. Electrophysiological monitoring and permeability studies are used, which are both reliable measures of endothelial layer permeability.

Method: Human umbilical vein endothelial cells (HUVEC) were cultured on ultrasound (US) transparent membranes. The cell cultures were positioned at a distance of 60 mm from the unfocused single-element transducer. The temperature of the medium was kept constant at 37°C. US exposure consisted of bursts with a frequency of 1 MHz, a length of 10.000 cycli, a P_ of 245 kPa and a repetition rate of 20 Hz. BR14 microbubbles, which consist of gas microbubbles encapsulated in a phospholipid-shell, were added in a microbubble-cell ratio of 1:1. The total experiment time was 2 minutes. Electrophysiological monitoring (TransEndothelial Electrical Resistance, TEER) was done using an Endohm-24 chamber coupled to an EVOMX meter. Normal TEER levels of the HUVEC cells were compared to the levels in cells treated with BR14 plus US. Further, permeability was quantified by measuring the transport of a 69 kDa macromolecular marker (albumin) across the HUVEC layer.

Results: TEER studies showed that BR14 plus US were able to decrease TEER values to 70 % of the initial values, indicating the ability of BR14 plus US to compromise the integrity of the cell layer. Controls (US alone, BR14 alone or no treatment at all) did not decrease TEER values. BR14 plus US increased albumin transport by 10% when compared to the controls. Microscopic examination revealed that all cells were still present on the membrane after the treatment and no significant amount of cells had died.

Conclusion: This study reveals the ability of insonified microbubbles to influence the endothelial layer integrity. Manipulating cell layer permeability results in lower TEER and higher transport of macromolecules. This study is the beginning of revealing the mechanisms involved in increased endothelial layer permeability by means of ultrasound and contrast agents.

Acknowledgments: The BR14 samples were provided by Bracco Research SA. This project is supported by innovation subsidies collaborative projects by the Dutch Ministry of Economic Affairs under number IS042035.

Physical Parameters Affecting Ultrasound/Microbubble-Mediated Gene Delivery Efficiency

Ahad Rahim[1], Sarah L. Taylor[1], Nigel L. Bush[2], Gail R. ter Haar[2], Jeffrey C. Bamber[2] and Colin D. Porter[1]

The Institute of Cancer Research, [1]Section of Cell and Molecular Biology, 237 Fulham Rd., London SW3 6JB [2] Joint Department of Physics, The Institute of Cancer Research and The Royal Marsden NHS Trust, Downs Road, Sutton, SM2 5PT UK

Gene delivery mediated by ultrasound in combination with microbubble contrast agents is a promising technology with potential advantages suited to clinical application, specifically the specificity achievable by means of dependence on ultrasound exposure of the target site after systemic (ideally) vector administration. Previous studies have shown that transfection can be achieved but many are unsatisfactory in regards to the exposure apparatus, the lack of definition of the ultrasound field or limitations imposed on the parameter space that can be explored by virtue of the use of clinical ultrasound machines. Thus, there is no clear understanding of factors influencing gene delivery. To address the need for establishing the influence of individual exposure parameters as a key step in advancing this technology we have assembled a system minimising experimental artefact and allowing control of many parameters of the ultrasound field. Using a 1MHz transducer we have varied parameters such as the ultrasound pulse amplitude, length and repetition frequency, the overall duration of exposure, and the microbubble and DNA concentrations to optimise delivery of naked plasmid DNA. Delivery of a plasmid coding for nuclear-localised β-galactosidase was achieved, using commercially-available lipid microbubbles (SonoVue®) and clinically acceptable ultrasound exposures, to adherent cells at efficiencies of ~4%. The exposure factors (and their optimal values) most significantly affecting efficiency with minimal impact on cell survival were the acoustic pressure amplitude (0.25 MPa peak-negative), pulse length (40 cycles), pulse repetition frequency (1kHz) and microbubble concentration (4% by volume). Both the pressure amplitude and the pulse length were important, and are known to be determinants of microbubble cavitation, but there was also some dependence on pulse repetition frequency. Total exposure duration as short as 10s, (corresponding to a time averaged ultrasound energy per unit area as low as 0.83J/cm^2) was just as effective as longer exposures. These data are the first in terms of thoroughness in exploring individual effects of various ultrasound exposure parameters for gene delivery. This study will be the basis for more-informed approaches to developing clinical applications of ultrasound/microbubble-mediated gene delivery.

How ultrasound and microbubble mediated gene delivery modalities influences gene delivery efficiency in endothelial cells.

Bernadet D. M. Meijering, Rob H. Henning, Wiek H. van Gilst, Leo E. Deelman

Department of Clinical Pharmacology, University Medical Centre Groningen, A. Deusinglaan 1, 9713 AV Groningen, Netherlands

Currently, gene therapy is still in the experimental phase, as gene therapy has not been approved for regularly use in the clinic by regulatory authorities so far. In about 70% of the clinical gene therapy trials viruses are used. Viruses have the natural ability to infect host cells and hence comprise a very efficient method to deliver and express genes in cells. However, a major drawback of viral gene transfer are immunogenic, cytotoxic and oncogenic responses. Because of these unwanted effects, there is an increase in research focusing on non viral application methods, such as the transfer of plasmids with the aid of ultrasound and microbubbles. One of the main problems of non viral vectors is their limited efficiency in gene delivery and expression. The aim of this study was to develop an efficient Ultrasound and microbubble (US&M) mediated gene delivery protocol.

In our studies, we used an *in-vitro* set-up in which all ultrasound parameters could be well controlled. An optimisation protocol was designed in which several parameters were systematically changed, including the number of US pulses, plasmid DNA concentration, ultrasound frequency and timing of removal of microbubbles following US exposure. Bovine aorta endothelial cells were seeded into Opticells. Sonovue microbubbles were incubated with plasmids containing the reporter genes GFP and Luciferase for several minutes, before addition to the endothelial cells. Then cells were exposed to US with an MI of 0.28 in 50 msec blocks of 1.000-10.000 pulses. After 24 hours, gene delivery was evaluated for efficiency by luciferase activity measurements and for side-effects by quantification of cell death.

Figure 1 shows how several factors in US&M mediated gene delivery influence transfection efficiency. An increase of US pulses up to 7000 pulses resulted in an increase in luciferase activity, whereas the use of 10.000 pulses resulted in a decrease in luciferase activity. This decrease in luciferase activity at the highest number of pulses is probably due to a severe increase in cell death. Another major increase of about 8-fold in luciferase activity was found when the incubation time after US exposure with transfection medium containing microbubbles was reduced from 16 to 0 hours. Furthermore, a 1.7 fold increase of gene delivery efficiency was found when the US exposure time was reduced from 2 minutes to 30 seconds of US exposure.

When DNA concentration was decreased, a rapid decline in luciferase activity was observed. Higher concentrations of DNA increased the luciferase activity in the areas exposed to US, but also resulted in transfection outside the US targeted area.

Finally, a change in US frequency from 2.25 MHz to 1 MHz resulted in a reduction of the gene delivery efficiency by 50%.

Our studies provide insight in how several factors influence the efficiency of US&M mediated gene delivery. In all, changes resulted in a 34 fold increase of efficiency compared to our primary protocol. At present, the functionality of US&M mediated delivery of therapeutic genes is being evaluated in an *in-vivo* model of oxidative stress. Further, our optimized protocol for US&M mediated gene delivery will be used to transfect blood vessels in an *ex-vivo* setup.

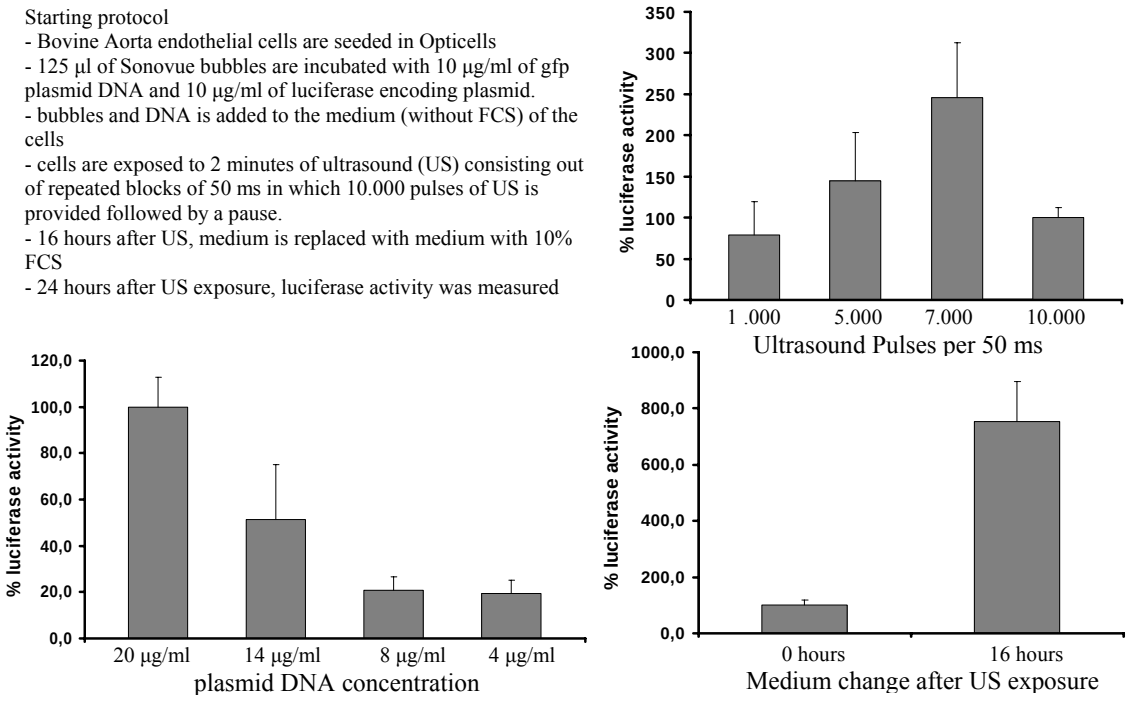

Figure 1. *Factors influencing ultrasound and microbubble mediated gene delivery effciency. Factors were systematically changed. Most effective condition is then changed in the protocol and is set to 100% luciferase activity.* ***A.*** *initial protocol.* ***B.*** *ultrasound pulses per 50ms changed parameter in initial protocol, N≥6.* ***C.*** *change in DNA concentration, N≥7.* ***D.*** *medium change after ultrasound exposure, N≥8.* ***E.*** *time of ultrasound exposure, N≥6.* ***F.*** *Ultrasound frequency, N≥4 .*

Microbubbles for Mouse Imaging

S.P. Stapleton, E. Cherin, R. Williams, P.N. Burns and F.S. Foster

Imaging Research - Sunnybrook and Womens College Health Sciences Centre
Toronto, Canada

Introduction: Ultrasound studies in the 20-40 MHz range exploit the widespread use of mouse models for pre-clinical investigation of human disease. The ability to resolve structures on the order of tens of microns has led to the visualization of the microvasculature[1] and the *in vivo* assessment of the effects of anti-angiogenic drug treatment in mouse tumour models[2]. These studies also demonstrated a low sensitivity to slow flow and structures below 40 micron for frequencies in the range of 20-40 MHz, which could be improved using microbubble contrast agents. This motivates the investigation of microbubble imaging techniques for use in small animal imaging. Three main considerations are explored for small animal imaging using microbubble contrast agents: 1) agent concentration; 2) optimal imaging parameters for non-linear detection methods; and 3) the disruption threshold for microbubbles.

Microbubble generated contrast is dependent on agent concentration or dose. The dose used to achieve an optimal contrast effect in humans does not directly translate to a similar contrast effect in small animals. When selecting an optimal dose for small animal imaging it is important to consider physiological parameters such as metabolic rate and blood volume. As well, it is important to consider changes in exposure conditions when the frequency is increased from 1-10 MHz to 20-40 MHz. First, the specific metabolic rate of a mouse is roughly seven times greater than for a human[6]. This could result in a higher elimination rate of contrast agent in a mouse versus a human. Second, the specific blood volume of a human is greater than in a mouse[6]. Achieving a similar contrast agent dilution in blood, or bubble haematocrit, will require modifying the contrast agent dose used in humans to get a similar agent dilution in mice. Finally, the width of the ultrasound beam is much narrower at frequencies in the 20-40 MHz when compared to the 1-10 MHz range. This results in fewer microbubbles in the ultrasound beam and consequently a lower backscattered signal. Therefore it is important to characterise the backscatter intensity as a function of microbubble dose.

Non-linear properties of microbubble contrast agents exposed to 1-10 MHz ultrasound frequencies provide a significant increase in contrast for human imaging[3, 4, 5]. However, these techniques cannot simply be scaled to obtain a similar contrast effect for smaller animals at higher ultrasonic frequencies. Microbubbles become less resonant as the frequency increases.

While it has been demonstrated that a subpopulation of microbubbles do exhibit non-linear behaviour when exposed to ultrasound in the 20-40 MHz range, this technique has a relatively high variability[7].

Therefore optimal imaging parameters for efficient non-linear echo production from microbubbles exposed to high frequencies needs to be investigated.

Microbubbles can be disrupted when exposed to significant pressures. Knowledge of the disruption threshold dictates what pressure levels are required for efficient non-linear imaging. Image contrast can be severely degraded in the presence of microbubble destruction due to loss of signal. As well, controlled agent destruction is important for disruption-replenishment imaging and drug delivery techniques. While it has been shown that microbubble destruction is dependent on several imaging conditions such as frequency, pressure and number of cycles[8] in the 1-10 MHz range, little is known about the mechanisms and levels of disruption in the 20-40 MHz frequency range.

The objective of this study was to experimentally investigate the potential for microbubble disruption of a commercially available contrast agent in the 20-40 MHz range. This was accomplished by determining microbubble disruption sensitivity as a function of pressure and number of cycles.

Materials and Methods: A solution of degassed water containing a 0.01% concentration of Definity^{TM} was flowed through a tissue mimicking phantom containing a 1 mm vessel. A flow rate of 6 mm/s was used. A transducer was placed near the inflow of the vessel and used to disrupt the agent. The microbubbles were exposed to a range of pressures (0.68-3.63 MPa) and number of cycles (1, 10, 20) and a transmit frequency of 20 MHz. A frame rate of 30 Hz was used for all measurements. At this frame rate an average number of 10 pulses hit the microbubble as it flowed through the sensitive volume. The amount of agent disruption was measured downstream using a second transducer operating at 40 MHz. B-mode cineloops were recorded before and during exposure to the destruction pulses. Raw backscattered signal from the agent was simultaneously collected and digitized at 200 MHz by an A/D board (DP210, Acqiris, Switzerland). A measure of disruption was estimated by taking the normalized ratio of the integrated power spectrum calculated from the raw data pre and post disruption, this is termed the normalized disruption ratio.

Results: Figure 1 shows the effects of disruption at 20 MHz, 3.63 MPa, 20 cycles and 30 frames per second. Clear indication of microbubble destruction is evident. Parabolic flow is observed as the microbubbles flow back into the field of view.

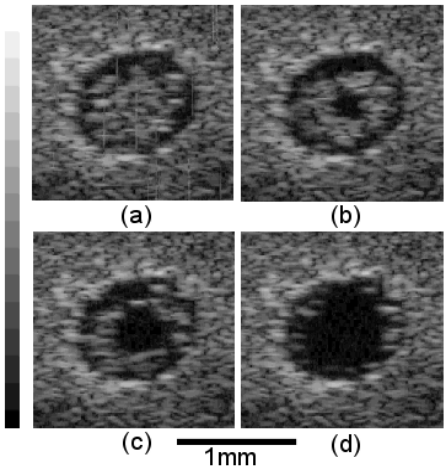

Fig. 1. Evolution of disruption at 20 MHz with a pressure of 3.6 3MPa, 20 cycles, and 30 frames per second.

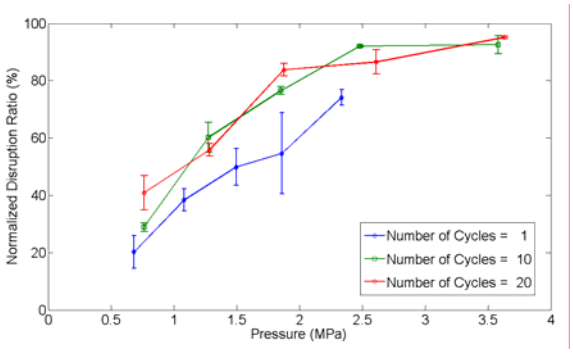

Fig. 2. Normalized disruption ratio as a function of pressure and pulse length. The disruption frequency is 20 MHz at 30 frames per second.

Figure 2 suggests that a subpopulation of microbubbles detectable at 40 MHz can be disrupted at 20 MHz. This figure shows that at moderate pressure levels (700 kPa), the disruption ratio ranges from »20% to 40% depending on the pulse length. As the pressure increases the amount of disruption increases to a point where almost all bubbles detectable at 40 MHz are destroyed. Figure 2 also shows the effect of different pulse lengths. There is a 10% difference in the disruption ratio between 1 cycle and 10 cycles for low pressures (<1 MPa). As the number of cycles increases from 1 to 20 an increase in the disruption ratio of 20% is found. Between 1 and 2 MPa the amount of disruption observed for 1 cycle remains approximately 20% less than the amount measured for 10 and 20 cycles. Above 2 MPa it appears that the amount of disruption at 1 cycle is comparable to the level observed for 10 and 20 cycles. Over the entire pressure range the difference in the amount of disruption between 10 and 20 cycles is negligible. These results indicate that at pressures below 2 MPa disruption can be minimized by pulsing with fewer cycles. However, when the number of cycles exceeds 10 then the amount of disruption is dominated by the pulse amplitude. A clear distinction between disruption as a function of number of cycles is seen when the pressure is less than 1 MPa. Therefore, further investigation of microbubble disruption in the 100 kPa to 1 MPa range is required. While a clear disruption threshold isn't evident from these data, it can be seen that a pressure of 1.0 MPa and 10 or 20 cycles or a pressure of 1.5 MPa and 1 cycle is required to eliminate approximately 50% of the detected signal from the microbubbles.

Conclusion: Results indicate that a significant amount of disruption is possible at 20 MHz. Work is currently in progress to translate these results to *in vivo* applications. Disruption will be characterised *in vivo* by measuring the integrated power spectrum pre and post disruption in the mouse liver and kidney. Future work will also determine the optimal microbubbles concentration and the pressure levels required for efficient non-linear and disruption-replenishment imaging. Knowledge of microbubble behaviour *in vivo* in the 20-40 MHz frequency range is necessary for quantitative interpretation of contrast flow studies. This project will lay the foundation for non-invasive longitudinal small animal haemodynamic measurements using high frequency ultrasound and microbubbles.

References

[1] D.E. Goertz, D.A Christopher, J.L. Yu, R.S. Kerbel, P.N. Burns and F.S. Foster, ”High-frequency color flow imaging of the microcirculation,” *Ultrasound Med. Biol.*, vol. 26, no. 1, pp. 63-71, 2000.
[2] D.E. Goertz, J.L. Yu, R.S. Kerbel, P.N. Burns and F.S. Foster, ”High-frequency Doppler ultrasound monitors the effects of antivascular therapy on tumour blood flow,” *Cancer Res.*, vol. 62, no. 22, pp. 6371-6375, 2002.
[3] P.N. Burns, ”Ultrasound contrast agents in radiological diagnosis,” *Radiol. Med.*, vol. 87, no. 5, suppl. 1, pp. 71-82, 1994.
[4] D.H. Simpson, T.C. Chien, and P.N. Burns, ”Pulse inversion Doppler: a new method for detecting nonlinear echoes from microbubble contrast agents,” *IEEE Trans. Ultrason. Ferroelect. Contr.*, vol. 46, pp. 372-382, Mar. 1999.
[5] K. Wei, A.R. Jayaweera, S. Firoozan, A. Linka, D.M. Skyba, and S. Kaul, ”Quantification of myocradial blood flow with ultrasound-induced destruction of microbubbles administered as a constant venous infusion,” *Circulation*, vol. 97, no. 5, pp. 473-483, 1998.
[6] K Schmidt-Nielson, ”Scaling: Why is animal size so important?,” Cambridge University Press, London, 1984.
[7] D.E. Goertz, S.W.S Wong, E. Cherin, C.T. Chin, P.N. Burns and F.S. Foster, ”Non-linear scattering properties of microbubble contrast agents at high frequencies,” *Proc. IEEE Ultrason. Symp.*, pp. 1747-1750, 2001.
[8] J.E. Chomas, P. Dayton, D. May, and K.W. Ferrera, ”Threshold of fragmentation for ultrasounic contrast agents,” *J. Bio. Opt.*, vol. 6, no. 2, pp. 141-150, 2001.

The use of ultrasound contrast agent is mandatory during real-time 3D stress echocardiography

A Nemes, ML Geleijnse, TW Galema, OII Soliman, WB Vletter, FJ ten Cate

Department of Cardiology, Thoraxcentre, Erasmus MC, Rotterdam, The Netherlands

Introduction: Recent studies have demonstrated the clinical usefulness of ultrasound contrast agents (CA) in the enhancement of endocardial border detection during dobutamine stress echocardiography (DSE). The purpose of the present study was to evaluate the quality of wall segment visualisation during real-time 3-dimensional echocardiography (RT3DE) with and without the use of CA.

Methods: The patient population consisted of 18 subjects who underwent stress RT3DE. A standard 17-segment model of the left ventricle was used during RT3DE. For visualization of each wall segment, a 4-grade scoring model was used: not available, poor, moderate and good.

Results: The visualization of 306 left ventricle wall segments was analysed at baseline conditions and during the peak stress with and without contrast. The numbers of segments are presented in the Table.

	At rest CA-	**At rest CA+**	**p**	**At peak CA-**	**At peak CA+**	**p**
not available	27	6	**<0.001**	97	5	**<0.001**
poor	75	28	**<0.001**	87	30	**<0.001**
moderate	117	65	**<0.001**	60	96	**<0.001**
optimal	87	207	**<0.001**	62	175	**<0.001**

Conclusions: Although RT3DE is a new promising tool for DSE, the use of a contrast agent is mandatory for optimal evaluation of wall motion.

The Role of Contrast-Enhanced Ultrasound Prior to Percutaneous Focal Liver Lesions Biopsy

Wei Wu[1], Min-Hua Chen[1], Shan-Shan Yin[1], Kun Yan[1], Ying Dai[1], Zhi-Hui Fan[1], Wei Yang[1], Ling Huo[1], Ji-You Li[2]

1 Department of Ultrasound, School of Oncology, Peking University, 52 Fu-cheng Rd, Beijing 100036, People¡¯s Republic of China.

2 Department of Pathology, School of Oncology, Peking University, 52 Fu-cheng Rd, Beijing 100036, People¡¯s Republic of China.

Purpose: To evaluate the clinical utility of contrast-enhanced ultrasound in percutaneous focal liver lesion biopsy.

Methods: One hundred and eighty-six (186) patients with focal liver lesions detected either by ultrasound or contrast-enhanced computed tomography (CT) were randomly divided into 2 groups, contrast-enhanced ultrasound group (CEUS group) and ultrasound group (US group). CEUS group (79 patients, 129 lesions) underwent SonoVue contrast-enhanced ultrasound (CEUS) prior to biopsy and US group (107 patients, 143 lesions) did not undergo CEUS prior to biopsy. Conventional ultrasound (US) was used in all patients to guide the biopsy procedures. The pathological diagnosis was considered definitive and final if the biopsy result was malignant. If the initial biopsy result was benign or negative for malignancy, then the result was either confirmed or denied based on contrast-enhanced CT, magnetic resonance imaging (MRI), angiography, serum alpha-fetoprotein (AFP) or clinical follow-up over a period of 6 months. In some patients with suspected malignancy, biopsy was repeated when conside red necessary during the follow-up. The diagnostic accuracy of the initial biopsy was defined as the percentage of the total number of lesions that were correctly diagnosed at the initial biopsy. The difference in diagnostic accuracy between the 2 groups was analyzed to evaluate the value of CEUS prior to biopsy.

Results: Of the 129 lesions in CEUS group, 28 (21.7%) were benign and 101 (78.3%) were malignant. Of the 143 lesions in US group, 36 (25.2%) were benign and 107 (74.8%) were malignant. There was no significant difference in the distribution of malignant and benign lesions in these 2 groups ($p>0.05$). There was no statistically significant difference in the lesion size distribution between CEUS Group and US group. (¦Ö2=0.619, $p>0.05$). The diagnostic accuracy of the initial biopsy was significantly higher in CEUS group than in US group (95.3% vs. 87.4%, $p<0.05$). The diagnostic accuracy of the initial biopsy for malignant lesions ¡Ü 2.0 cm in size was also significantly higher in CEUS group than in US group (97.1% vs. 78.8%, $p<0.05$). No major complications occurred in our study except one case of pneumothorax in US group.

Conclusion: CEUS prior to percutaneous focal liver lesion biopsy improved the diagnostic accuracy of this procedure by providing important intra-lesion information for differentiating viable, denaturalized or necrotic tissue and consequently providing more accurate information on the site of biopsy even in lesions ¡Ü 2.0 cm and reduced the number of puncture attempts.

Key Words: Ultrasonography, Percutaneous, Biopsy, Contrast-enhanced Ultrasound, Liver tumors

On the mechanisms of cell membrane permeabilization with ultrasound and microbubbles

T. A. Tran[1-3], S. Roger[2-3], J.Y. Le Guennec[2-3], F. Tranquart[1-4], A. Bouakaz[1-3]

2. Inserm, E0211, 37000 Tours, France ;
1. Inserm, U619, 37000 Tours, France;
3. Université F. Rabelais, Tours, France.
4. CIT Ultrasons, Tours, France

Aim: New clinical applications of ultrasound contrast agents extend beyond imaging and diagnostic towards therapeutic applications. A number of experimental findings have now demonstrated evidence of increased cell membrane permeability through sonoporation process. In this study, we explore the mechanisms by which the activation of microbubbles with ultrasound waves modulate cell membrane permeability.

Method: An electrophysiological experimental method is set up to explore the cell membrane response in sonoporation conditions. This experimental method consists of measuring the variations in membrane potential which directly indicates the modulation of ion exchange through the cell membrane and thus its conductance. To measure the cell activity during sonoporation, patch clamp technique was used in the "whole cell" configuration where the membrane potential of a single cell is measured. Mammary cancer cells issued from MDA-MB-231 cell-lines were used. Sonovue microbubbles provided by Bracco Research were continuously infused to the cells at a rate of 1ml/min. Ultrasound was applied using single element transducers of 1 and 2.25MHz, both focused at 14 mm. Waveforms of different lengths (20 to 40 cycles), amplitudes (50 to 400 kPa), repetition rates (100 to 500 μs) and exposure times (5 to 20 sec) were transmitted. The microbubbles and cells were simultaneously monitored during ultrasound exposure using a video camera.

Results: The results revealed that during sonoporation, a marked hyperpolarization of the cell membrane potential occurs during the ultrasound excitation, indicating the triggering of specific ion channels while the cell and the bubble remain viable. At the highest acoustic exposure (pulses of 40 cycles at 1 MHz repeated every 100 μs during 20 sec); the membrane potential varied from about -30 mV (resting value) to -60 mV and this phenomenon was entirely reversible. This mechanism showed to be dependent on the number of contrast microbubbles in the close vicinity of the cell, but revealed that only cells in direct contact with the bubbles undergo membrane hyperpolarization. Smaller acoustic amplitudes induced only mild hyperpolarization (less than 20mV) while shutting off the ultrasound brings the potential to its resting value. Ultrasound alone does not affect the cell membrane potential.

Since oscillating microbubbles induce changes in plasma membrane shape in the contact area, a mechanical pressure was applied on the cell using a glass probe. A similar hyperpolarization, of 17 ± 1.9 mV amplitude (n=5 cells), was observed. The hyperpolarizations induced by ultrasound activated microbubbles and by the glass probe were inhibited by iberiotoxin (10^{-7} M), a specific inhibitor of potassium (BK_{Ca}) channels. Therefore we propose that one mechanism for enhanced permeability of cell membrane by ultrasound-activated microbubbles is the increased of BK_{Ca} conductance.

Conclusions: The results demonstrate that microbubbles' oscillations under ultrasound activation entail modifications of the electrophysiological cell activities, by triggering the modulation of ionic transports through the plasmic cell membrane. However, only cells in a direct contact with the microbubbles are impacted. The involved mechanisms are related to activation of specific channels sensitive to mechanical stresses (stretch-activated channels) and possibly non-specific ion channels.

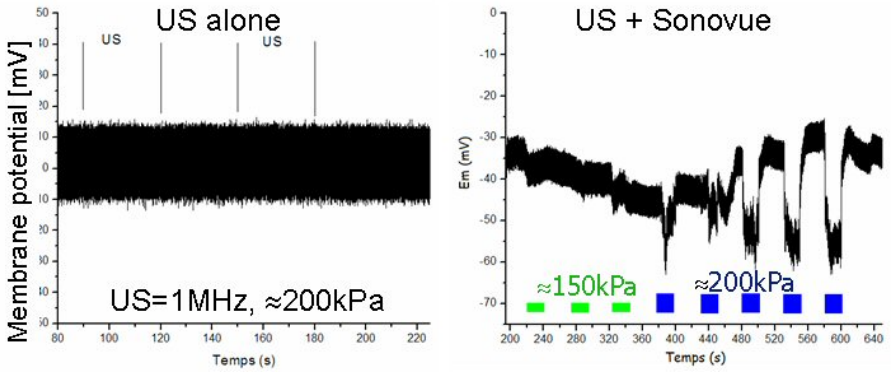

Acoustic response of shrinking bubbles

Peter D. Bevan[1,2], Raffi Karshafian[1,2], and Peter N. Burns[1,2]

[1]Department of Medical Biophysics, University of Toronto, Toronto, Canada
[2]Sunnybrook & Women's College Health Sciences Centre, Toronto, Canada

Bubble disruption is an important phenomena associated with the response of ultrasound contrast agents (UCAs) exposed to high acoustic pressures. At a high enough pressure, the same sound that is used diagnostically to image these microbubbles can be used break their shell, releasing the gas inside. This behaviour is important both for bubble detection and imaging techniques as well as proposed therapeutic applications and drug delivery schemes.

Previous work in our lab has measured, acoustically, the disruption threshold and post-disruption echo from populations of microbubbles (Bevan, et al., 2004). This suggested a model for UCA disruption whereby ultrasound breaks the shell, leaving free gas bubbles. Over time, these free gas bubbles slowly disappear into the surrounding liquid. Diffusion of gas causes the bubbles to shrink and, consequently, reduces in the measured backscattered echo over time. Parts of this physical picture have been verified through correlation with optical measurements on the same bubbles (Bouakaz, et al., 2005). The work presented here is a theoretical framework to describe this behaviour along with a comparison to experimental measurements.

A model is used in which the size of a given bubble over time is calculated by the method of Epstein and Plesset (1950) which describes how the size of a spherical gas-filled cavity in liquid changes over time. The response to a 2MHz, broadband, 35kPa peak-negative-pressure pulse is calculated by numerical solution of the differential equation presented by Keller and Miksis (1980). Following dispruption, the bubble is taken to be free gas in water. The combination of these two processes is used to derive the echo from a single bubble as it shrinks.

In order to calculate the response from a *population* of bubbles, 40 bubbles, whose sizes are chosen randomly from a known distribution, are placed at random positions in the region of interest (ROI) of the simulation. The echo from each bubble in the ROI is summed as a function of time, with some bubbles shrinking (after supposed shell disruption) and others remaining the same size. The size threshold for disruption is decided according to the optical measurements of Chomas, et al. (2001), who measured the disruption thresholds for individual lipid-shelled bubbles as a function of acoustic pressure and bubble size.

The backscattered echo power vs. time curves calculated using this model are used to predict the values of two parameters: (1) the reduction in echo power between 1 and 200ms post-disruption and (2) the decay time of the echo vs. time curve, as measured by the time constant of a monoexponential decay fit to the data. For several lipid-shelled bubbles tested to date, the model predictions are consistent with the experimental results with respect to the drop in backscatter power. The decay time, reflected in the time constant of the fit, however, is overestimated by the model, especially at higher pressures.

Recent optical observations of disruption of lipid-shelled bubbles (e.g. Postema & Schmitz, 2005) demonstrate that lipid-shelled bubbles tend to *fragment* into many smaller bubbles on disruption. It would be expected, then, that these smaller bubbles will disappear more quickly, resulting in a faster decay time. Fragmentation has been added to the model proposed here by dividing the gas, by volume, randomly into newly-formed bubbles at the same spatial location as the original bubble. This addition to the model brings the theoretical predictions much closer to the measured experimental values.

Future work pursues two avenues of investigation. First is to improve the model to predict the behaviour of bubbles containing different gasses and with different shell types. Second is to characterize the post-disruption behaviour of clinical UCAs experimentally over a range of pressures, frequencies and other acoustic conditions, for which data can then be compared to the predictions of the model.

References

Bevan PD, Karshafian R, Matsumura M, Tickner G, and Burns PN. *An acoustic study of disruption of polymer shelled bubbles.* IEEE International Ultrasonics Symposium. Montreal, Quebec, Canada, 2004.

Bouakaz A, Versluis M, and de Jong N. *High-speed optical observations of contrast agent destruction.* Ultrasound in Med. Biol., 31(3)391-399, 2005.

Chomas JE, Dayton P, May D, and Ferrara K. *Threshold of fragmentation for ultrasonic contrast agents.* J. Biomed. Optics, 6(2)141-150, 2001.

Epstein PS and Plesset MS. *On the stability of gas bubbles in liquid-gas solutions.* J. Chem. Phys, 180(11)1505-1509, 1950.

Keller JB and Miksis M. *Bubble oscillations of large amplitude*. JASA, 68(2)628-633, 1980.

Postema M and Schmitz G. *Ultrasonic fragmentation of microbubbles: a theoretical approach of the flash in flash-echo.* Proc. IEEE Eng. in Med. and Biol., Shanghai, China, Sept. 1-4, 2005.

Acknowledgement

The authors would like to acknowledge the contribution of Dr. Alexander Klibanov for providing the microbubbles measured in these experiments. This work was supported by the Terry Fox Programme of the National Cancer Institute of Canada and the Canadian Institutes of Health Research.

Contrast Quantification of Flow:
Compensating for the non-uniform ultrasound beam profile

John M. Hudson, Raffi Karshafian, Peter N. Burns

Medical Biophysics, University of Toronto, Canada

Introduction: Ultrasound contrast agents are used to measure blood flow and blood volume by exploiting the ability of microbubbles to be disrupted, then preferentially detected with bubble specific imaging techniques. Tissue flow is measured by using the ultrasound imaging beam to disrupt freely flowing microbubbles within the scan plane with a short burst of ultrasound energy. This creates a regional 'void' of tracer which then re-fills with contrast at a rate dependent on the flow and reaches a final asymptotic value dependent on the blood volume of the feeding vasculature—this is the method of disruption/replenishment [Wei, 1998]. Since its inception, the replenishment-time curve is generally fitted to a mono-exponential function that can be criticized as lacking a fundamental physiological basis. While the replenishment technique in its current form might be used to quantify the *relative* flow rate and vascular volume of a given system, its reproducibility and accuracy in a clinical setting remains low, inhibiting its widespread adoption. This is partially due to the inadequacy of existing physical models that are used for analysis to account for some of the more subtle details of the technique and its dependencies. It has been shown that the actual form of the replenishment-time curve is a reflection of both the hemodynamics and the structural organization of the vasculature that is contained in the region of interest [Karshafian, 2003]. This has motivated the development of more appropriate models to describe the replenishment-time curve that are founded on physical principles [Arditti et al, 2004].

One example is that the ultrasound beam, which defines the volume of interrogation, is not uniform in both the scan and elevation planes and in practice depends on parameters that include the location of maximum pressure (focus), the physical dimensions of the transducer (aperture) and tissue attenuation. The problem is compounded in the context of contrast flow measurements because the spatial pressure distribution of the beam is related in a nonlinear way to the measured microbubble signal. As a result, the measured signal intensity of a homogenous vascular system is seen to vary with interrogation depth. In addition, the difference in the pressure distributions between the high MI disruption beam and the low MI detection beam effectively defines two distinct regions (Figure 1), a phenomenon that is reflected in the replenishment-time curve. Accounting for these effects is an initial step towards improving quantitative flow and volume measurements with ultrasound contrast agents.

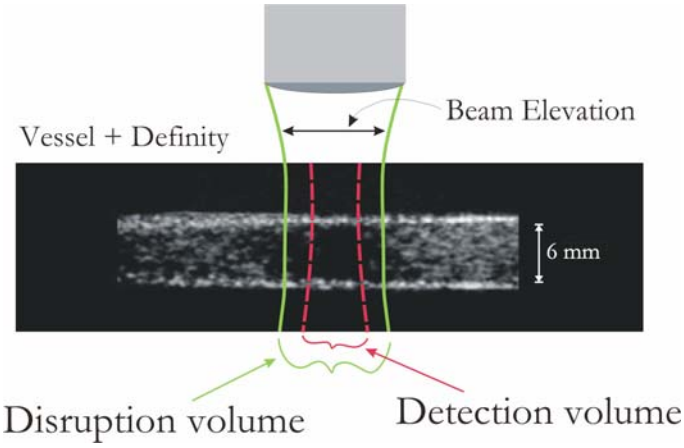

Figure 1: *Microbubble disruption in a single tube. The disruption and detection regions differ in size.*

In this work, a single vessel flow phantom with a 3D positioning system was used to investigate the effects of a non-uniform ultrasound beam profile on microbubble disruption-replenishment quantification. A simple physical model was developed to describe the expected replenishment signal. Together, the phantom and model are used to investigate and compensate for the difference between the high and low MI disruption/detection boundaries as well as the depth-dependent signal intensity.

Model: The single pipe flow model is based on a continuous polynomial velocity profile through a single straight tube. We assume that the high MI disruption beam creates a sharp boundary whose borders lay beyond that of the detection region, which responds with a uniform sensitivity (Figure 2).

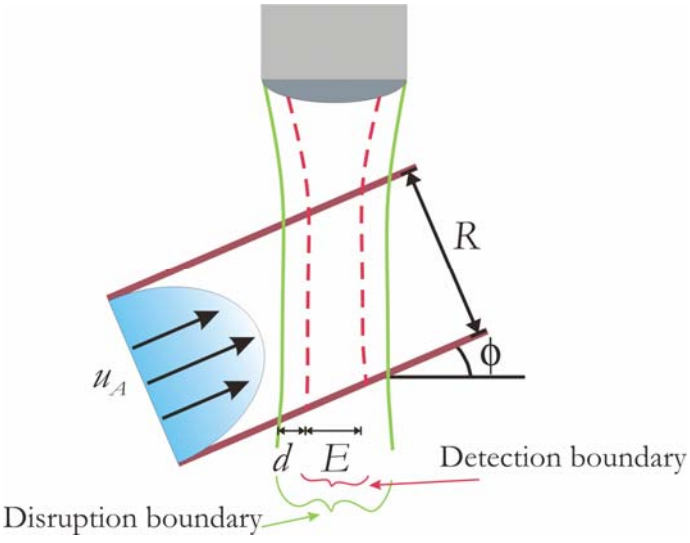

Figure 2: *Pictorial representation of the in vitro system with a polynomial velocity profile (2D cross section). The mathematical model considers aspects of both the flow system itself (radius, mean velocity) and details of the ultrasound beam (detection width E and disruption delay width d).*

The replenishment-time signal in a single vessel with a 3D polynomial velocity profile (Figure 2) is described by the piece-wise function

$$S(t)=\begin{cases} 0, & 0\le t\le \dfrac{d}{u_m\cos\phi} \\ \pi R^2\left(\dfrac{u_m t}{2\cos\phi}-\dfrac{d}{\cos\phi}+\dfrac{d^2}{2u_m t\cos\phi}\right), & \dfrac{d}{u_m\cos\phi}\le t\le \dfrac{E+d}{u_m\cos\phi} \\ \pi R^2\left(\dfrac{E}{\cos\phi}-\dfrac{(E+d)^2}{2u_m t\cos\phi}+\dfrac{d^2}{2u_m t\cos\phi}\right), & \dfrac{E+d}{u_m\cos\phi}\le t\le\infty \end{cases} \qquad (1)$$

where S is the signal intensity, t the elapsed time, R the radius of the vessel, u_m the mean velocity, ϕ the angle between the ultrasound beam and flow direction, E the width of the detection boundary and d the difference in distance between the detection and disruption boundaries.

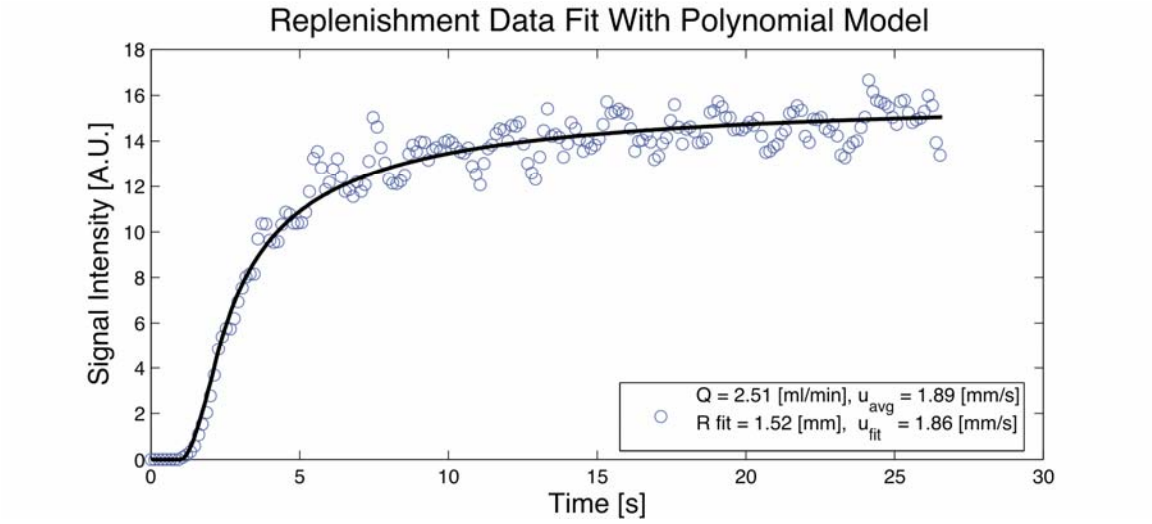

Figure 3: *Experimentally measured signal intensity as a function of time of microbubble replenishment through a single vessel. The data* (o) *is fit* (–) *with the polynomial model of Equation 1. Q and* u_{avg} *are the independently measured flow rate and average velocity through the tube. R and* u_{fit} *are the radius and mean velocity derived from the fit. With the proper selection of the detection width E and delay d, the experimental data and theory are well matched.*

Experimental Method: The flow phantom is composed of a series of wall-less vessels of diameters between 3-6 mm, surrounded by a tissue mimicking Agar/Carbon mixture with an attenuation range of 0-0.2 [dB/cm/MHz]. Contrast enhanced ultrasound loops of RAW data were acquired with a clinical ultrasound system (Toshiba Aplio) at 6MHz (transducer-PLT604AT) and analysed offline (CHI-Q) for a range of flow rates (0.010-0.020 [ml/min]), microbubble/degassed water concentrations (Definity, 0.010-0.020 [ml/l]) and imaging depths. The width of the detection boundary was estimated with a lab-made resolution phantom as well as by direct visualization *in situ* with a second clinical ultrasound system operating at low MI (see Figure 1).

Results and Discussion: Figure 3 demonstrates the significance of these two regions for a given flow rate, where we see a clear time delay between the beginning of replenishment and the onset of the signal rise. Incorporating this effect as a parameter in the model is required to ensure a good fit. Additionally, the width of the detection/disruption boundaries exhibit a strong dependence on interrogation depth, owing to the position of the ultrasound focus, beam shape and attenuation. Thus any attempt to properly model replenishment must take into account these variable characteristics on a depth specific basis. There is also evidence of a velocity dependence on the delay parameter *(d)* that becomes more significant at lower flow rates. This may be relevant in a clinical setting when regions of vasculature that include both fast and slow velocities through large vessels and capillaries are examined.

The single tube phantom and the flow model presented here have been developed as a tool to investigate fundamental dependencies of the disruption/ replenishment technique. This work illustrates the need to correctly identify/characterize both the detection and disruption boundaries for proper curve fitting and accurate velocity quantitation. Consideration of additional physical properties, such as a 'fuzzy' or non-abrupt disruption boundary (due to varying disruption thresholds within a real bubble population), the ultrasound's nonlinear sensitivity to a distribution of microbubble sizes as well as the relationship between the measured signal intensity and bubble concentration is required to better understand and properly apply the disruption/replenishment technique. Furthermore, the advent of real-time contrast enhanced 3D ultrasound will require the extension of the ideas presented here to include multiple vessels and multiple flows in a real 3D network.

References:

Arditti M, Frinking P, Zhou X, Rognin N & Messager T, "A new formalism for the destruction-replenishment perfusion assessment technique based on physical considerations", *9th Symposium on ultrasound contrast imaging,* Erasmus, Rotterdam, [2004]

Karshafian R, Burns PN, Henkelman MR, "Transit time kinetics in ordered and disordered arterial trees", *Phys Med Biol,* vol 48, pp. 3225-37 [2003]

Wei K, Jayaweera AR, Firoozan S, *et al.* "Quantification of myocardial blood flow with ultrasound-induced destruction of microbubbles administered as a constant venous infusion", *Circulation*, vol 29, pp. 1081-88 [1998]

Contrast Specific Spatial Compounding

Christian Hansen [1,2], Nils Hüttebräuker [2], Mohammad Ashfaq [2], Wilko Wilkening [1], Helmut Ermert [1,2]

[1] Ruhr Center of Excellence for Medical Engineering (Kompetenzzetrum Medizintechnik Ruhr, KMR)

[2] Institute of High Frequency Engineering, Ruhr-University Bochum, Bochum, Germany

Purpose: In a project of the Ruhr Center of Excellence for Medical Engineering at the Ruhr University Bochum, Germany, a system was developed for ultrasound computed tomography of the female breast. A high precision mechanical system was realized to implement a tomography system around a commercial ultrasound scanner. Using this setup, both, reflection mode (e.g. pulse-echo) and transmission mode are feasible. In transmission mode acoustic parameters like speed of sound and attenuation can be reconstructed, and these parameters are reported to be related to breast cancer [1] [2]. Other important diagnostic parameters are perfusion and vascularization, which can be imaged using contrast agents. For the experiments presented here, phase inversion RF data was acquired in reflection mode to generate a 360° compound scan of a flow mimicking phantom with contrast agent. Spatial compounding achieves an isotropic resolution, reduces speckle and artefacts and may have a diagnostic value in the context of breast imaging [3].

Methods:

Data Acqusition:

A Siemens Sonoline Antares was used to generate compound scans of a flow mimicking phantom in a water tank. The scanner was set up to image in phase inversion mode (i.e. tissue harmonic imaging, THI) and with low MI. Two probes were consecutively mounted into the tomographic applicator: a curved array C5-2 (center frequency: 3.5 MHz, transmit frequency: 2 MHz, transmit power: 2.5 % of maximum power, displayed MI: 0.3, single focus, scan lines: 180, density: 4.24 lines/degree) and a linear array VF10-5 (center frequency: 7.5 MHz, transmit frequency: 4.21 MHz, transmit power: 5.0 % of maximum power, displayed MI: 0.4, single focus, scan lines: 360, line density: 94 lines/cm). In combination with this system the Axius Direct Ultrasound Research Interface (URI) was used to obtain unprocessed, beamformed RF data with 16 bit resolution and 40 MHz sampling rate [4].

The transducer was rotated about the object by a computer controlled servo-motor (72 angular positions for a whole revolution) whilst data acquisition was triggered with the ECG module over the LPT port of the same PC. For each position of the probe one THI frame was stored to be downloaded afterwards to the PC via local area network (LAN). Figure 1a gives a schematic overview of this setup. The applicator was calibrated and the center of rotation was evaluated with the help of a polypropylene fiber phantom by means of the techniques proposed in [5].

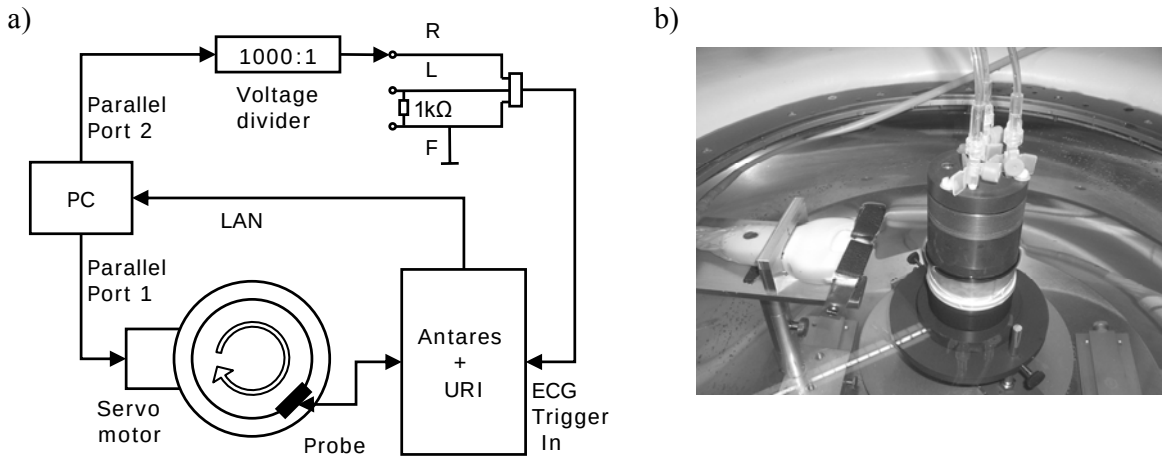

Figure 1: *a) Schematic sketch of the experimental setup.*
b) Ultrasound CT setup: Transducer installed in the water filled tank in front of the flow mimicking phantom.

Flow Phantom:

A polyvinyl alcohol phantom (i.e. cryogel) was constructed as shown in figure 1b. While the upper and lower parts of this phantom were held by two plastic casings, the middle part was fully exposed to allow a 360° compound scan. Inside the phantom, three capillary ducts (diameter: 0.8 mm) were fed with water and contrast agent, respectively, from an elevated reservoir by three flexible tubes and cannulae. A fourth duct was generated as a reference without being supplied. Two measurements were carried out with each transducer: one without contrast agent, the other with 2.5 ml Sonovue mixed in 10 l of water. With this setup the flow rate was high enough to ensured that contrast agent was exchanged completely between frames.

Data Analysis:

THI mode images were generated by adding together the phase inversion echo pairs prior to envelope detection to eliminate the first harmonic. Scan conversion and rotation of the demodulated images to their respective angles of incidence was conducted simultaneously to generate a compound scan. The scan conversion accounts for refraction that is due to the difference in speed of sound between the phantom and the surrounding liquid (water: 1490 m/s; phantom: 1529 m/s, measured before and assumed to be uniform). Refraction was considered by computing ray paths according to Snellius law and aligning the individual A-lines along these paths [6].

Results: Figure 2a and 2b show THI images from data obtained with the curved array (left: without contrast agent, right: with contrast agent). The upper bright spot in both images (white box) is the non-supplied duct. The other three ducts are only visible in the THI image with contrast agent (white arrows).

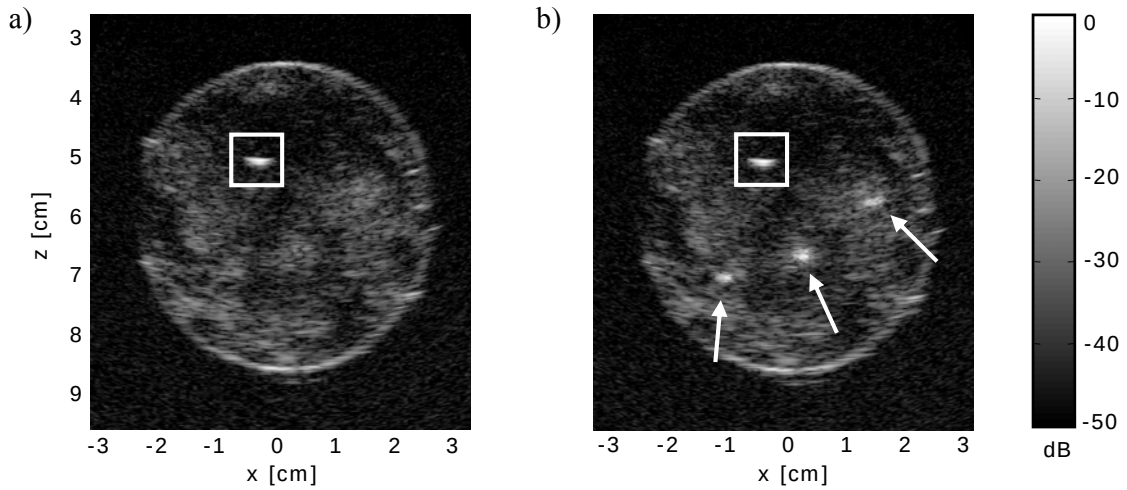

Figure 2: *Standard THI images without contrast agents (a) and with contrast agents (b). Both images are standardized to the maximum intensity of the image with contrast agent. The white box depicts the non-supplied duct, whereas white arrows show the supplied ducts.*

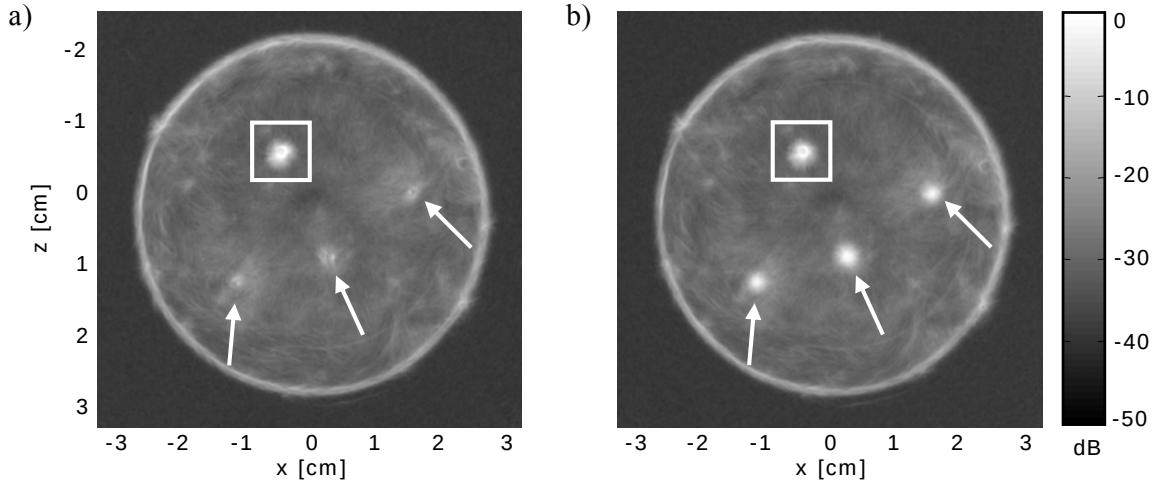

Figure 3: *Compound images from THI data without contrast agents (a) and with contrast agents (b). Both images are standardized to the maximum intensity of the image with contrast agent. The white box depicts the non-supplied duct, whereas white arrows show the supplied ducts.*

Figure 3a and 3b show the respective compound images obtained as described above. One can see that in these images artefacts are reduced. Darker areas, for instance, disappear, if they do not result from morphology but from differences in tissue harmonics due to the respective angle of the incident wave. Furthermore, speckle noise is decreased so that even in the image without contrast agent the three ducts supplied with water are visible (white arrows) next to the non-supplied duct (white box). However, in the image obtained using contrast agent the three supplied ducts appear bright and can better be seen than in the standard THI counterpart. Subtracting both images from each other, a baseline or blank value subtraction can be conducted. Figure 4b shows results after such a subtraction.

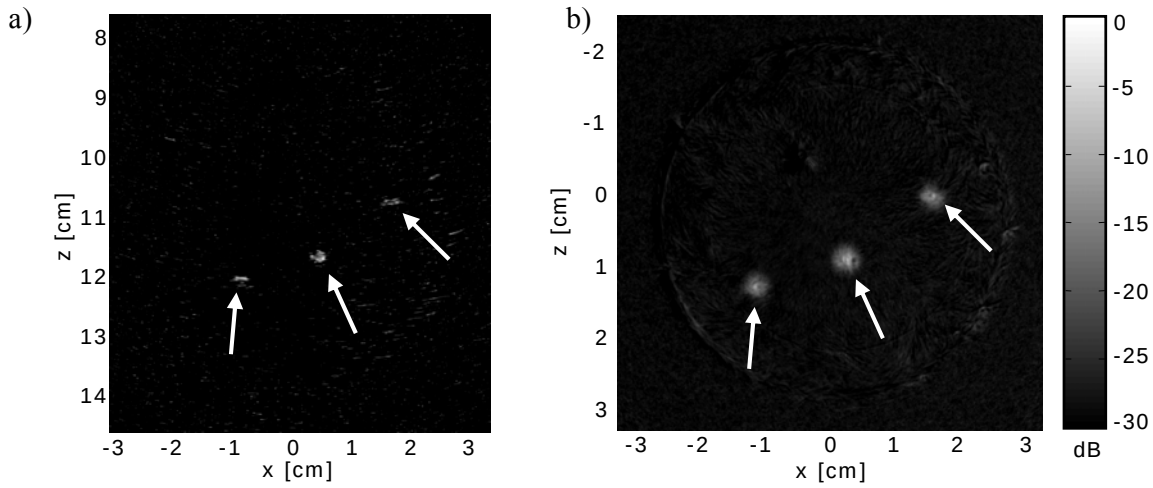

Figure 4: *Images after baseline subtraction computed from Standard THI images (a) and from compound images (b). White arrows show the supplied ducts.*

Here, only the ducts supplied with contrast agent remain. The afore visible non-supplied duct and the solid parts of the phantom disappear completely. This technique yields better results for compound images than for standard THI-mode images (see figure 4a) since in the latter speckle noise and an anisotropic resolution affects the image quality.

Conclusion and Outlook: In this paper, we presented initial results of spatial compounding with ultrasound contrast agents. With this approach a subtraction angiography without speckle appears to be possible. As both echoes of THI data are acquired, morphology can be described, in addition, by an artefact and speckle free B-mode compound image processed from the same data. Next to the presented compound technique, which yields an averaged gray value for each pixel, a maximum intensity compounding is possible as well. While the former shows an image weighted by blood volume and flow rate, the latter can be used to image vascular structures. Future work will comprise techniques to quantify perfusion parameters like flow rate and blood volume (e.g. depletion or replenishment method). In a next step, volume data sets will be generated with the same setup by scanning several image planes upon each other.

Acknowledgements

This work is a project of the Ruhr-Center of Excellence for Medical Engineering (Kompetenzzentrum Medizintechnik Ruhr, KMR), Bochum, Germany. It is funded in part by the Federal Ministry of Education and Research, Germany (BMBF), grant 13N8079. We would like to thank Siemens Medical Solutions, Inc. for additional support.

References:

[1] Ashfaq, M., Ermert, H.: *A new approach towards ultrasonic transmission tomography with a standard ultrasound system*. IEEE 2004 Ultrasonics Symposium Proceedings (2004), P2U-M-6.

[2] Ashfaq, M., Ermert, H.: *Ultrasound Spiral Computed Tomography for Differential Diagnosis of Breast Tumors using a Conventional Ultrasound System.* Acoustical Imaging, Vol. 27 (Arnold, W., ed.), Kluwer Academic / Plenum Publisher, New York (2003), pp. 627-633.

[3] Huber, S, Wagner, M., Medl, M., Czembirek, H.: *Real-time Spatial Compound Imaging in Breast Ultrasound.* Ultrasound in Medicine & Biology 28 (2) (2002), pp. 155-163.

[4] Brunke, S., Insana, M., Dahl J., Hansen, Ch., Ashfaq, M., Ermert, H.: *An Ultrasound Research Interface for a Clinical System.* IEEE Trans Ultrason Ferroelect Freq Contr, 2006, accepted.

[5] Jago, J. R.: *An Automated Method for determining the centre of rotation of a mechanically scanned reflection UCT System.* Phys. Med. Biol., Vol. 39, (1994), pp. 2367-2371.

[6] Ashfaq, M., Hüttebräuker, N., Hansen, Ch., Wilkening, W., Ermert, H.: *Spatial Compounding with Tissue Harmonic Images and Monostatic Aperture Reconstruction*. Proceedings of 2005 IEEE International Ultrasonics Symposium (2005), in press.

Optical investigation revealing pressure threshold for the onset of ultrasound microbubble oscillations

M. Emmer[*1,2], *J. Borsboom*[1], *A. van Wamel*[1], *M. Versluis*[2], *and N. de Jong*[1,2]

Dept. of Experimental Echocardiography, Thoraxcentre, Erasmus MC, Rotterdam, the Netherlands,
[2]*Physics of Fluids, University of Twente, Enschede, the Netherlands*

Background*:* Next to enhancing microbubble stability, the bubble shell also strongly influences its oscillating behaviour. In previous optical studies [1], we have shown that in contradiction to the predictions of current models, microbubbles with similar sizes can respond differently to ultrasound insonification. We hypothesize that by adding a shell to the microbubble, threshold and hysteresis effects are introduced, which have a certain influence on the dynamic behaviour of microbubbles. In order to get more insight in the contribution of the shell upon the microbubble oscillating behaviour, we investigated threshold and hysteresis effects in individual microbubbles using high-speed imaging.

Method: To investigate these effects, two experiments were carried out. Both experiments used the experimental phospholipid encapsulated agent BR14 (Bracco Research SA, Geneva, Switzerland). It was insonified at 2 MHz centre frequency. Images of individual microbubbles were recorded with the Brandaris-128 camera system [2] at a frame rate of 14 million frames per second. The acoustic pressure threshold for bubble oscillation was investigated through recording individual bubbles in twelve sequences of 64 image frames. A single bubble was insonified with twelve cycle sine wave bursts with increasing peak pressures (40 - 300 kPa) in subsequent sequences. For the hysteresis effect, we recorded sequences of 128 frames in which a single bubble was exposed to a Gaussian apodised burst with a full width at half maximum duration of 3.5 μs and a peak pressure of 300 kPa.

Results: In the threshold experiment, it was observed that only bubbles of larger than 3 micrometers in diameter oscillated for pressures up to 60 kPa. For pressures up to 200 kPa, bubbles larger than 1.5 micrometers oscillated. For pressures up to 300 kPa, bubbles larger than 1.2 microns were observed to oscillate. When comparing single bubble responses between the ascending and descending side of the Gaussian burst, we observed that most of the microbubbles above or below resonance size had higher radial amplitudes at the ascending side. The radial amplitude as a function of acoustic pressure of these bubbles described a clockwise hysteresis curve.

Conclusions: Current models do not fully capture the dynamic behaviour of encapsulated microbubbles. Smaller encapsulated microbubbles do not oscillate until the acoustic pressure has exceeded a threshold value, which is inversely related to the initial bubble size. In addition, we found a hysteresis effect in most of the responses of non-resonant bubbles. These findings may have implications in novel detection methods.

1. Postema, M., et al., *Simulations and measurements of optical images of insonified ultrasound contrast microbubbles.* IEEE Trans. Ultrason., Ferroelect., Freq. Contr., 2003. **50**(5): p. 523-536.
2. Chin, C.T., et al., *Brandaris 128: a 25 million frames per second digital camera with 128 highly sensitive frames.* Rev. Sci. Instru., 2003. **74**(12): p. 5026-5034.

Non-linear Corruption of Ultrasound Transmission by Microbubble Contrast Agents

Meng-Xing Tang* and Robert J. Eckersley**

**Wolfson Medical Vision Laboratory, Department of Engineering Science,*

Oxford University, Oxford, UK

***Imaging Sciences Department, Faculty of Medicine, Imperial College London, London, UK.*

In this paper a source of artefact in contrast enhanced ultrasound imaging has been described and investigated. The artefacts arise due to non-linear corruption of the propagating ultrasound pulses as they propagate through regions containing microbubble contrast agents. Current techniques for detection of microbubble contrast agents are based on the detection of nonlinear components of the echoes, however, the bubbles along the transmission path between transducer and target can contribute to the nonlinearity of the echoes and consequently introduce imaging artefacts, especially in regions at depth. This not only induces changes in the echoes from bubbles causing errors in image intensity but also results in nonlinear echoes from linear scatterers leading to misrepresentations of linear scattering structures as bubbles. In this paper we identify and provide insight into the non-linear corruption caused by microbubble contrast agents and the effects on current nonlinear imaging techniques. The corruption is investigated through both simulation and experimental measurements. Significant imaging artefacts are identified when detection techniques deploying multiple insonation pulses, such as pulse inversion and combined phase and amplitude modulation are used. The study reveals that the corruption of an ultrasound pulse involves nonlinear amplitude attenuation, phase change, and addition of new harmonic components during the transmission by forward scattering, all of which are dependent on the initial insonating acoustic pressure. The amplitude and phase corruption are less sensitive to initial insonating phase if long pulses are used where bubbles are more likely oscillate in steady states, as opposed to transient oscillations brought on by shorter insonating pulses.

Laser Tweezers for manipulation and control of Ultrasound Contrast Agents

Valeria Garbin[1,2], Dan Cojoc[1], Enrico Ferrari[1,2], and Enzo Di Fabrizio[3]

[1]TASC National Laboratory, INFM-CNR, S.S. 14 km 163.5, 34012 Trieste, Italy
[2]Department of Physics, University of Trieste, via Valerio 2, 34027 Trieste, Italy
[3]Magna Græcia University of Catanzaro, Campus di Germaneto (CZ)

Studies of the fundamental aspects of ultrasound contrast agents dynamics are hampered by buoyancy and bubbles clustering; bubbles are not easily observed when they are free to oscillate away from interfaces and neighboring bubbles. In this work we present a setup for manipulation and control over bubbles position which enables studying bubbles dynamics with controlled, repeatable boundary conditions.

Micro bubbles are trapped with laser tweezers, a powerful tool for non-contact, non-destructive manipulation on the micro scale. Laser beam shaping enables to trap not only single bubbles, but also multiple bubbles in a suitable configuration, for studying bubble-bubble interaction.

Radial Modulation Imaging: A dual frequency ultrasound imaging technique for microbubble contrast

Hamid H. Shariff [1,2], Peter D. Bevan[1,2], Raffi Karshafian[1,2], Michael Karakolis[2], Milan Banerjee [2], Peter N. Burns[1,2]

1. Department Medical Biophysics, University of Toronto, Toronto, Canada

2. Sunnybrook and Women's collage Health Sciences Centre, Toronto Canada

Introduction: Microbubbles have been successfully used to image blood flow at the tissue level using nonlinear pulse-echo techniques such as harmonic and pulse inversion imaging, which are widely available in modern clinical ultrasound scanners (1). One fundamental issue limiting further progress is that whereas linear imaging scales with frequency, microbubble imaging does not, as it is linked to the radial resonance of a bubbles with a more or less fixed size. Satisfactory high frequency, high resolution imaging using microbubble contrast agents has therefore not yet been achieved. In this work, we examine the feasibility of 'Radial Modulation Imaging' (2) a dual frequency imaging technique that decouples the imaging frequency from the bubble resonant frequency, allowing the former to be raised, so improving spatial resolution.

Principles and Methods: A bubble driven by ultrasound below its resonance frequency will oscillate out of phase with one driven above its resonance frequency. This property is exploited for bubble detection by continuously driving the bubble below its disruption threshold at a frequency near resonance; this is the 'modulating' source. A second source of sound is used for conventional pulse-echo imaging at a higher frequency, with the pulses synchronized to insonate the bubble at the points of peak expansion and peak compression due to the modulating wave.

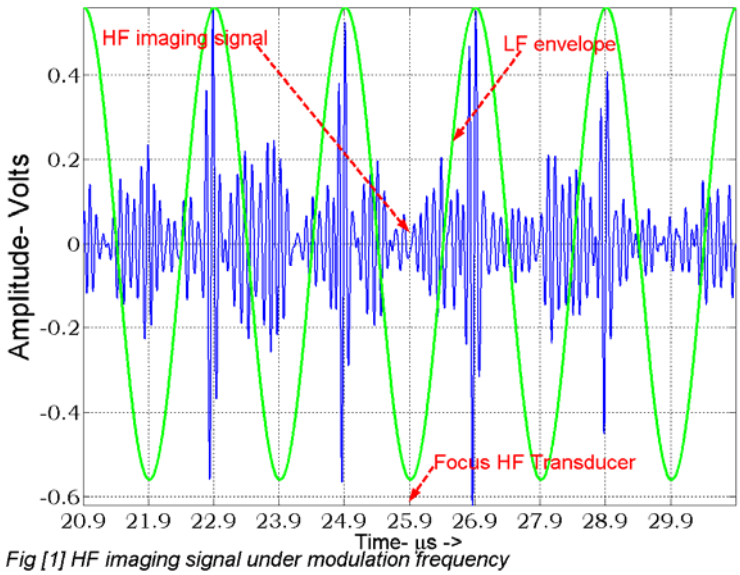

The two resulting echoes are then subtracted. Echoes from linear scatterers, which are unaffected by the modulating wave, cancel. Those from the bubble combine additively over the entire bandwidth of the imaging pulse. In this experiment, proof of principle is investigated by means of two transducers perpendicularly aligned and overlapping at their respective foci

in a flowcell containing the microbubble contrast agent DefinityTM at a concentration 0.01ml/l. A 500kHz-modulating frequency (10 cycles cosine tapered, Pneg=130kPa, MI=0.19,) was used to change the radius of bubbles and a 10 MHz detection pulse (3-cycles Gaussian, Pneg=190kPa, MI=0.06) was used to probe the echo response of the bubbles at the peak of rarefaction and compression phases. A series of six high frequency detection pulses placed 1ms apart were used in the pulsing scheme. The first two pulses in the scheme were transmitted in the absence of the modulating wave and provided pre-modulation control data. The modulation was turned on for the third and fourth pulses, which interrogated the bubble at the peak of rarefaction and compression phases respectively of the modulating frequency. The last two pulses were again controls in the absence of the modulating wave, and revealed effects such as bubble disruption, which can easily confound an experiment such as this. Echoes at the imaging frequency were acquired from the flowcell and bandpass filtered for analysis.

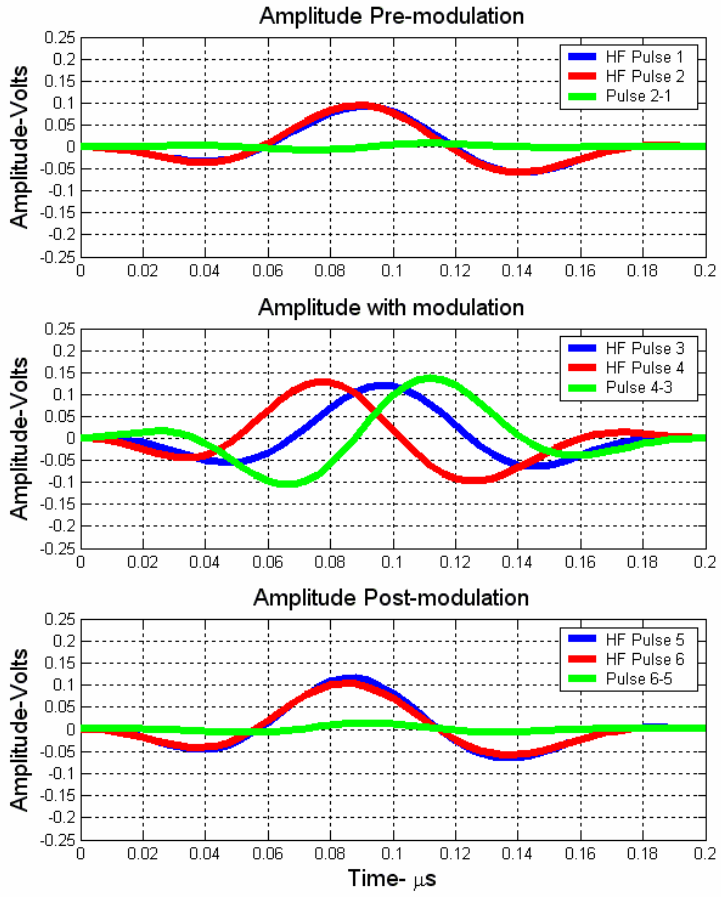

Fig [2], Phase incoherence with modulated microbubbles

Results: As shown in Figure [1], the bubble echo from the peak of the compression phase of modulation (green trace), where bubbles reached their minimum radius, was very strong. In contrast, the echo from the peak of the rarefaction phase of modulation, where bubbles reached their maximum radius, gave a much weaker response.

The reason for this observation is not entirely clear, but it is in agreement with that observed by Bouakaz et al (3), using high speed optical observation of a comparable setting, with 500 kHz modulated bubbles insonated at 3.5 MHz. Figure [2] (top) shows that the subtraction of high frequency signals from unmodulated microbubbles in pulse 1 and 2 resulted in almost complete cancelation (green trace), whereas the difference signal between pulses 3 and 4, with radial modulation, (Figure [2] middle) resulted in a strong contrast signal (green trace). (Figure [2] bottom) shows two coherent signals from the last pulses without modulation, demonstrating that the bubbles are intact.

Further experiments were also carried out with an agar gel phantom containing graphite particle s as a tissue mimicking material, replacing the microbubbles in the flowcell. The difference between imaging pulses was measured in the presence of the modulating wave.

Figure [3] compares these results (mean±SD) with those from the bubbles in 10 repetitions of the experiment for a range of peak negative pressures of the modulating pulse from 40-200kPa. At 200kPa, the RMS amplitude of the radially modulated bubbles was found to be approximately 32 dB higher than the signals from the agargraphite phantom. It should be noted that the radial modulation signal, unlike those from most nonlinear techniques, contains the full bandwidth of the bubble echo.

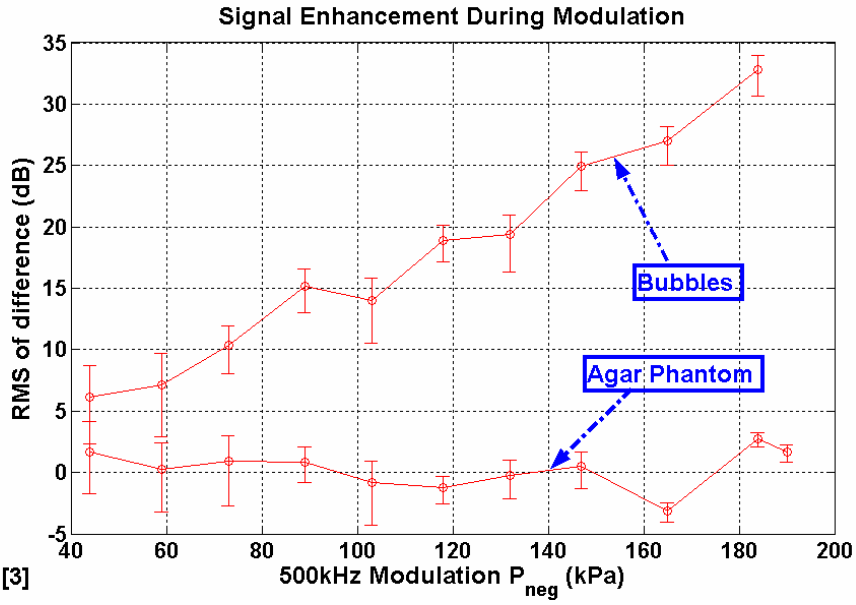

Fig [3]

Conclusions

Our experiments demonstrate that the radial modulation technique is a feasible method for bubble-specific imaging, which may address the problem of effective nonlinear methods for higher frequencies. In these experiments, the contrast-to-clutter ratio increased with peak pressure of the modulating signal, reaching a peak of 35dB. Future work will focus on specific implementations with Doppler and *in vivo* measurements.

Acknowledgement

This work was supported by the Terry Fox Programme of the National Cancer Institute of Canada and the Canadian Institutes of Health Research.

References

1. Hope Simpson D, Chin CT, Burns PN. Pulse Inversion Doppler: A new method for detecting nonlinear echoes from microbubble contrast agents. IEEE Transactions UFFC 1999; 46:372-382.

2. Hansen R, Angelsen B, Bouakaz A, Borsboom J, Versluis M, deJong N, Burns PN. Radial modulation imaging. In: tenCate F, deJong N, eds. Ninth European Symposium on Ultrasound Contrast Imaging. Book of Abstracts. Rotterdam: Erasmus Univ, 2004.

3. Hansen R, Johansen TF, Burns PN, Angelsen BAJ. Contrast Agent Detection through Low Frequency Manipulation of High Frequency Scattering Properties. IEEE UFFC Ultrasonics Symposium. Montreal, 2004.

Current Ultrasound Contrast Imaging Methods and the Future Ahead

M. Averkiou[1], M. Bruce[2], S. Jensen[2], J. Powers[2], P. Rafter[2], T. Brock-Fisher[2]

[1]University of Cyprus, [2]Philips Medical Systems

In eleven years of *European Symposia on Ultrasound Contrast Imaging* we went from very limited understanding of microbubble physics and no clinical utility of the images produced, to truly understanding contrast microbubbles to the point where we load them with drugs and making clinical images in both cardiology and oncology on a daily basis. The main property of bubbles that drove the contrast imaging research is *nonlinearity*. In the last 4-5 years multi-pulse schemes have been widely accepted as the method of choice. Even though there are a plethora of names and techniques available today they all do the same task: they extract differential nonlinear response between two or more states while suppressing linear tissue response. Some of the techniques developed in chronological order are pulse inversion, power modulation, a combination of pulse inversion and power modulation, harmonic coded excitation, difference frequency imaging (including radial modulation imaging and subharmonic imaging), and pulse subtraction imaging. To the physicist and engineer all of the above mentioned methods are very distinct and unique, to the more clinically inclined bio-physicist they are quite similar but perhaps still unique, and finally to the clinicians are all the same thing: they detect microbubbles while rejecting tissue.

All multi-pulse schemes do a great job of rejecting the tissue not only due to the fact that they detect the nonlinear response, but also due to the low amplitudes (MI) used to avoid bubble destruction. Pulse inversion produces the highest resolution images but suffers from sensitivity due to detection at the second harmonic and system electronics as the task to create two pulses that are perfect replicas of one another may be difficult. Power modulation and its hybrids/derivatives turned out to be one of the most reliable techniques thanks to its implementation. The transmit aperture is used in three (or more) consecutive firings where alternate elements that make half of the aperture or the full aperture are fired thus creating half and full amplitudes. In addition with power modulation, great sensitivity is achieved due to the fact that it also detects nonlinear energy at the fundamental where the tissue attenuation is lower. With difference frequency imaging (subharmonic imaging included) nonlinear mixing is utilized to place the received energy in the desired frequency range. Certain applications, e.g. high frequency, may benefit from this method. With the pulse subtraction technique, in addition to the nonlinearity, the dynamic transient nature of bubble is also utilized. The image resolution of these techniques seems to be adequate for the present and future clinical needs. The contrast sensitivity may need some further boost especially in cases like cirrhotic livers. It is the authors' belief that in future developments sensitivity gains in the order of 10 dB are both required and possible.

The physics of the imaging technique alone can not produce the image the clinicians require. There are a number of constraints that must be considered, both system specific and application specific, some of which are overall resolution, depth penetration, system and probe frequency response, dynamic range, frame rate, etc. In the recent years image processing schemes have also been employed to give more clinical information. One example is methods that are based on maximum intensity projection which offer better vessel visualization in both high and low vascularity scenarios by an approach that is almost equivalent to "infinite persistence". Names for these techniques are Microvascular Imaging (MVI) or MicroFlow Imaging. Applications for this approach span from breast oncology where low flows are hard to image, to liver oncology where vessel morphology is often used for diagnosis.

A natural progression of the imaging technology is the direction of live 3D contrast imaging. This is achieved with either motorized linear and curve-linear arrays or matrix arrays. The imaging techniques remain the same as with 2D imaging, and the main issue becomes presentation and visualization. Presentation of multiple orthogonal frames is one approach. Another is full volume scanning and then subsequent "slicing and dicing" to find the region of interest. Live 3D contrast imaging will lead us to two main future applications: image-guided oncology intervention and quantification of tumor angiogenesis. As tumor angiogenesis - the formation of new blood vessels and remodeling of the existing vasculature in a solid tumor - emerges as one of the principal targets for new therapeutic strategies in oncology, so the need has become evident for non-invasive means for its evaluation. And this need is only realizable with 3D ultrasound contrast imaging and an appropriate perfusion quantification approach.

The work presented here will review the current nonlinear microbubble imaging techniques and show clinical images to demonstrate their details. Emphasis will be placed on identifying the aspects of the images that relate to specific physical aspects of the technique used. Some initial work on 3D contrast imaging will be presented. Finally future needs for tumor angiogenesis imaging and quantification will be discussed.

Bubble behavior in capillaries

Kullervo Hynynen

Dept of Radiology, Brigham and Women's Hospital, Boston, USA

Most of the studies investigating gas bubble oscillations in sound field have been done in free fluid situations. However, when bubbles enter small blood vessels the fluid flow induced by the bubble oscillations will be influenced by the vessel walls and free fluid conditions are not adequate. This talk will review our results investigating the influence of the vessel size on the bubble resonance frequency and its collapse threshold. Both experiments with rigid tubes and simplified simulations indicate that the threshold of bubble collapse is increased by the reduced vessel size. This would indicate that there might be a preferential vessel size that would show the largest bio-effects when sonicated in the presence of preformed gas bubbles. Our recent electron microscopy study of rabbit brain demonstrated that arterioles had a higher concentration of marker molecule transport across the vessel wall than capillaries. Similarly, multi-photon in vivo microscopy observations of marker molecules in mouse brain showed vessel size dependence. In this talk our theoretical and experimental evidence will be summarized to try to start to understand the bubble behavior in small vessels and its potential impact on diagnosis and therapy.

Atomic Force Microscopy and microbubble science

E. Glynos[1], V. Sboros[2], S. D. Pye[3], C.M. Moran[2], M. Butler[2], J. Ross[4], W.N. McDicken[2], V. Koutsos[1].

[1]Institute for Materials and Processes, School of Engineering and Electronics, Centre for Materials Science and Engineering, University of Edinburgh, Edinburgh, UK. [2]Medical Physics, School of Clinical Sciences and Community Health, University of Edinburgh, Edinburgh, UK. [3] Medical Physics, Royal Infirmary of Edinburgh, Edinburgh, UK. [4] Clinical and Surgical Sciences, University of Edinburgh, Edinburgh, UK.

Microbubble modelling has limited predictive value and has not been of major assistance to microbubble science. The major unknown of these equations are the parameters related to the shell. Atomic force microscopy (AFM) is a versatile topograghy and mechanical nanosensor that can give spatial and force resolution of the order of Angstroms and subnanonewtons, respectively, and can be used to interrogate microbubbles manufactured for ultrasonic imaging.

Microbubbles were attached to the bottom of a Petri dish and were interrogated in saline. The Bioscope® AFM (Veeco, Santa Barbara, CA, USA) was used in tapping mode imaging to reveal topographical detail of biSphere® (POINT Biomedical Corp, San Carlos, CA, USA) microbubbles. As the microbubbles are of comparable size to the AFM cantilever tips, a convolution between the AFM tip and the microbubble resulted in the acquired topographies. Part of the top half of the bubble was imaged with lateral resolution around 30 nm and height resolution around 2 nm. Image analysis showed that the biSphere® can have typical root-mean-square roughness of around 80 nm, but peak-to-peak roughness is often above 0.5 μm .

The mechanical properties of the microbubbles were investigated using the Molecular Force Probe-1D (Asylum Research, Santa Barbara, CA, USA). We performed micro/nanocompression tests using the force-distance mode of the instrument. The range of compressive stiffness or effective spring constant for biSphere® was found to be between 1 and 10 Nm^{-1} using a cantilever with a spring constant of 0.6 Nm^{-1}. This stiffness was shown to decrease with the microbubble size. These results are also consistent with previous stiffness measurements using the Bioscope®. Measurements with Definity® (Bristol Myers-Squibb, N. Bellarica, MA, USA) microbubbles showed an order of magnitude less in stiffness (0.06-0.4 Nm^{-1}).

The adhesion properties of targeted microbubbles that use the streptavidin-biotin chemistry were also studied. Self-designed and manufactured lipid microbubbles were attached to tipless cantilevers that were previously treated in a poly-L-lysine suspension.

These attached microbubbles were then brought into contact with with SkHep-1 cells that were cultured in Petri dishes. Force-distance curves revealed multiple de-adhesion events upon retraction of a targeted microbubble from the cell. On the other hand, control microbubbles did not provide such behaviour. These results can be analysed to provide a bond analysis between the target cell and the microbubble.

In conclusion, the AFM is proposed here as an accurate tool for microbubble nanointerrogation.

Acknowledgement: The work was funded by the EPSRC (UK).

Contrast enhanced carotid vasa vasorum imaging: association between plaque echogenicity and neovascularization

Coli S, Magnoni M, Melisurgo G, Cianflone D, De Dominicis D, Marrocco-Trischitta MM, Chiesa R, Feinstein SB,* Maseri A.

*Dep. of Cardiothoracic and Vascular diseases, Vita-Salute University, San Raffaele Scientific Institute, Milan , Italy; *Rush University Medical Center, Chicago, USA*

Background: Feinstein and coworkers have recently provided initial evidence that contrast enhanced carotid ultrasound imaging can be used to study vasa vasorum and intraplaque neovascularization of carotid atherosclerotic lesions. Accordingly, we have started using contrast ultrasound to study the prevalence of these phenomenon in our population and correlate it with plaque echogenicity.

Materials and methods: We have studied 32 pts (27 males, age 68.9 ± 8.1 years) either referred for carotid endarterectomy or screened for carotid atherosclerosis after admission for ischemic heart disease in our department. All pts had at least one carotid stenosis >30%. Imaging was performed with a GE-Vivid 7, using a 7L probe. As 16 pts had 2 to 3 plaques because of bilateral and/or omolateral disease, globally 52 plaques were studied. Each plaque was classified in terms of echogenicity, during standard and compound imaging, according to a widely used classification scheme:

- Class I: uniformly echolucent
- Class II: predominantly echolucent
- Class III: predominantly echogenic
- Class IV: uniformly echogenic
- Class V: extensive calcification with acoustic shadowing

For contrast enhanced imaging Optison (GE) diluted in saline was injected in boluses; a low mechanical index (0.10-0.08) was used. Moving bright spots within the plaque or on its adventitial side were considered to represent bubble signal coming from plaque neovascularization. For each plaque contrast enhancement (neovascularization) was categorized as follows:

- Grade 0: no bubbles
- Grade 1: bubbles confined to plaque adventitial side and/or shoulder
- Grade 2: bubbles reaching plaque core
- Grade 3: extensive contrast enhancement throughout the plaque

Results: Plaques were quite evenly distributed among different classes (I 14%, II 21%, III 17%, IV 23%, V 25%) and some degree of neovascularization was found in nearly two third of the plaques (0: 37%, 1: 31%, 2: 17%, 3: 15%). When plaque class was plotted against neovascularization, more echolucent plaques were found to have a significantly higher degree of neovascularization ($p < 0.001$ by chi square for trend, fig.1). The results did not change when calcific (class V) plaques were excluded (fig.2). When plaque echogenicity and neovascularization were dichotomised (class I-II vs class III-IV-V, grade 0-1 vs grade 1-2), still a higly positive association was found between plaque echolucency and more intense neovascularization ($p < 0.001$ by chi square analysis, OR 11.6, 95% CI 3.0-45.4, fig.3). This association remained significant even after correcting for stenosis and patients having multiple plaques ($p <0.05$).

Conclusions: echolucent and predominantly echolucent plaques show a higher degree of neovascularization as shown by contrast enhanced carotid ultrasound. More echolucent plaques are known to have a higher risk of cerebrovascular events and a greater macrophage density. Neovascularization may be associated to plaque echolucency because this feature identifies more “active” plaques.

Combined Diagnostic & Therapeutic Ulrasound Transducer to improve Ultrasound Microbubble-Medical Thrombus Dissolution

Thomas Porter

University of Nebraska - Medical Center, Omaha, USA

Purpose. The effectiveness of intravenous microbubbles and therapeutic ultrasound (TUS) in recanalizing thrombosed vessels is reduced in the presence of significant tissue attenuation. This may be improved if TUS was applied only when these microbubbles were present within the thrombus. Simultaneous microbubble-sensitive imaging techniques could be used to detect these microbubbles and improve recanalization without the need for thrombolytics or anticoagulants.

Materials and Methods. In a chronic canine arteriovenous graft occluded by thrombus, TUS (1 MHz frequency, 10 W/cm^2 energy; 10% duty cycle) was applied through a six centimeter thick tissue mimicking phantom during an intravenous infusion of either saline (n=6 occlusions) or lipid encapsulated microbubbles (ImaRx Therapeutics; Tucson, AZ). TUS was intermittently applied during the microbubble infusion either at set time intervals (n=6 occlusions), or when simultaneous low-mechanical index (MI) diagnostic ultrasound imaging (Contrast Pulse Sequencing or CPS) detected microbubbles within the thrombus (n=12 occlusions). High MI diagnostic ultrasound (1.7 MHz at a mechanical index of 1.9 and duty cycle <1%) was also tested for thrombus dissolution using CPS as a guide. Success was defined as return of rapid flow within the graft (Grade 3 flow).

Results. Diagnostic ultrasound detected microbubbles moving through small channels within the thrombus prior to angiographic evidence of flow in the graft. This guided the timing of therapeutic ultrasound application better than using set time intervals. Angiographic clearance of thrombus and restoration of Grade 3 flow at 45 minutes of treatment were seen in 33% of thrombosed grafts treated with TUS and microbubbles at set time intervals, versus 92% of grafts treated with TUS guided by diagnostic ultrasound ($p<0.001$ compared to set time intervals). High MI diagnostic ultrasound used in conjunction with CPS to guide delivery had a similar efficacy restoring Grade 3 flow (75%).

Conclusion. The use of TUS or even high MI DUS with intravenous microbubbles has a high success rate in recanalizing deeply located thrombosed vessels when performed with simultaneous low mechanical index diagnostic ultrasound guidance.

Targeted Ultrasound Contrast Agents for Molecular Imaging in High-Shear Flow

A.L. Klibanov, J.J. Rychak, W.C. Yang, J.R. Lindner, B. Li, S. Acton, K.F. Ley.

University of Virginia, Charlottesville VA 22908

Targeted ultrasound contrast materials (gas-filled microbubbles carrying ligands to endothelial selectins or integrins) are evaluated as potential agents to image inflammation, ischemia-reperfusion injury or tumor angiogenesis. Antibodies against surface markers that are upregulated on the surface of endothelial cells are usually applied as targeting ligands immobilized on the bubble shell. Such microbubbles exhibit good targeting ability in the slow and medium flow conditions (under 1 dyne/cm^2 wall shear stress, such as in postcapillary venules). In the fast flow, in large arteries (relevant for vascular lesions such as atherosclerotic/vulnerable plaque), antibody-targeted bubbles would normally not be able to target efficiently to activated endothelium. Recently it was suggested that fast-binding ligands, such as a functional glycosulfopeptide 2-GSP-6 fragment of PSGL-1 protein, can be successfully used for microbubble targeting and retention in the high-shear flow conditions. Fast-binding ligands are applied by leukocytes to achieve slow rolling on activated endothelium in vivo, so the general microbubble bioengineering approach is to mimic natural leukocyte targeting. However, synthesis of glycosulfopeptide is complex. A simple non-antibody fast-binding ligand for microbubble targeting to P-selectin or E-selectin could be helpful for the design of ultrasound contrast materials for practical use. In this study we designed microbubble contrast capable of binding to targets in fast flow conditions (exceeding 4 dyne/cm^2 shear stress), by using clustered polymeric form of fast-binding ligand Sialyl Lewis X (P-SLex).

Microbubbles were prepared from decafluorobutane gas and stabilized with a monolayer of phosphatidylcholine, PEG stearate and biotin-PEG-lipid. P-SLex (biotinylated SLex polyacrylamide) or biotinylated anti-P-selectin antibody (RB40.34) was attached to microbubbles via a streptavidin spacer arm. *In vitro* testing of targeted binding was performed in a flow chamber by video microscopy: microbubble dispersion in PBS buffer was passed through a rectangular chamber formed by a rubber gasket and Lucite block inserted in a 35mm polystyrene dish. Microbubble targeting characteristics (sticking, rolling rates and pause times) were determined using Matlab-based custom image processing software. Polystyrene dish surface was coated with murine P-selectin at surface densities of 7 or 140 molecules/um^2, or E-selectin at 365 molecules/um^2. For ultrasound backscatter study, polystyrene plates coated with P-selectin and carrying P-SLex-microbubbles were placed in a water tank and interrogated using an ultrasound medical imaging system (Philips HDI 5000, L7-4 probe). *In vivo* studies were performed by intravital microscopy observation of microbubble targeting in a mouse cremaster muscle model.

In the parallel plate flow chamber, P-SLex bubbles demonstrated selective adhesion, retention or slow rolling on P-selectin-coated plates. Efficiency of firm targeted adhesion to P-selectin surface (at 140 molecules/um^2) was comparable for antibody-carrying bubbles and P-SLex-targeted bubbles at 0.68 dyne/cm^2 shear stress. At fast flow (4.45 dyne/cm^2), P-SLex-targeted bubbles maintained their ability to bind to the target firmly, while antibody-mediated targeting dropped more than 20-fold. At a lower surface density (7 receptor molecules/um^2), targeting via P-Slex was more efficient than via antibody in all the flow conditions tested. Targeting of P-SLex-targeted bubbles to E-selectin-coated surfaces was even more efficient than to P-selectin. Control plates, treated only with casein blocker, did not retain bubbles in the range of flow conditions studied.

P-SLex-targeted bubbles on P-selectin-coated plates were clearly visualized by ultrasound imaging with a clinical scanner; control plates lacking bubbles did not show significant acoustic backscatter.

In a murine cremaster muscle model efficacy of accumulation of intravenously administered SLex-polymer-microbubbles in the target tissue was comparable with targeting mediated by anti-P-selectin antibody, and exceeded the accumulation of non-targeted control bubbles by nearly 70-fold, most likely via targeting of PSlex to upregulated P- and E-selectin on vascular endothelium. Most of the targeted bubble accumulation in this model occurred in the slow flow vessels, such as postcapillary venules.

Conclusion. Polymeric Sialyl Lewis X, clustered on the surface of microbubbles at high ligand surface density, mediated selective targeting of ultrasound contrast on P-selectin and E-selectin-coated surfaces. Targeted bubbles could be visualized by ultrasound imaging. Binding in fast flow conditions improved considerably as compared with anti-P-selectin antibody-targeted bubbles. Targeted bubbles selectively accumulated *in vivo* in a mouse cremaster muscle model.

Clinical trials and clinical applications of Sonazoid in liver diseases

Fuminori Moriyasu, M.D.

The Fourth Department of Internal Medicine, Tokyo Medical University
6-7-1 Nishi-Shinjuku, Shinjuku, Tokyo, 160-0023

PURPOSE: Next generation ultrasound contrast agents are expected to act as both of vascular and Kupffer imaging. Clinical trial was performed to determine the clinical value of Sonazoid contrast enhanced ultrasound (CEUS) for the characterization during vascular phase and the detection during Kupffer phase of focal liver lesions, compared to unenhanced ultrasound (UEUS) and dynamic CT in patients with liver tumors.

METHOD and MATERIALS: 196 patients from 15 centers with known focal liver lesions were enrolled. There were 121 with HCC, 38 with metastasis, 17 with hemangioma, 9 with other benign tumors and 5 with other malignant tumors. All patients received fundamental, harmonic, color and power Doppler for vascular imaging and fundamental, harmonic for Kupffer imaging of UEUS. Sonazoid (0.12 micro-L Microbubbles/kg body weight) was injected intravenously. Contrast harmonic imaging targeted on the interested lesions was obtained during the first one minute after injection. The whole liver was scanned to detect lesions using a harmonic imaging ten minutes after injection as Kupffer imaging. Adverse events were followed for 72 hours. Each three blind readers for US and CT reviewed the images from UEUS, CEUS and dynamic CT, respectively.

RESULTS:

Characterization: 88.9% of the CEUS were correctly diagnosed by the blinded readers, although 68.4% of the UEUS were correctly diagnosed. There was statistically significant difference ($P<0.001$). Accuracy with dynamic CT was 88.2%. Diagnostic accuracy for hemangioma with CEUS was 100%.

Table 1 The accuracy, sensitivity and specificity of UEUS, CEUS and D-CT in characterization of malignant lesion(s) and benign lesion(s)

	Subjects	UEUS	CEUS	D-CT
Accuracy	190	164 (86.3)[a) b)]	185 (97.4)[a)]	180 (94.7)[b)]
Sensitivity	164	146 (89.0)[c) d)]	162 (98.8)[c)]	157 (95.7)[d)]
Specificity	26	18 (69.2)	23 (88.5)	23 (88.5)

a) McNemar test, $P<0.001$ (CEUS vs UEUS)
b) McNemar test, $P=0.005$ (D-CT vs UEUS)
c) McNemar test, $P<0.001$ (CEUS vs UEUS)
d) McNemar test, $P=0.016$ (D-CT vs UEUS)

Detection: The CEUS could find more lesions in the patients of 36.6% compared to the UEUS alone. There was statistically significant difference ($P<0.001$). The number of the lesions detected by the blind reviewers was increased in 31.9% of the patients with CEUS compared to the lesion number

reported from the enrolled site. It was 18.8% with dynamic CT and the difference was statistically significant (Wilcoxon, P<0.008).

Table 2 The detectability of UEUS, CEUS (post), CEUS (pre+post) and D-CT(%)

	Decrease	Agreement	Increase
UEUS[a)]	56 (29.3)	110 (57.6)	25 (13.1)
CEUS(post)[b)]	42 (22.0)	103 (53.9)	46 (24.1)
CEUS(pre+post)[a)b)c)]	29 (15.2)	101 (52.9)	61 (31.9)
D-CT[c)]	32 (16.8)	123 (64.4)	36 (18.8)

Wilcoxon signed-rank test
a) $p < 0.001$ (CEUS (pre+post) vs UEUS)
b) $p < 0.001$ (CEUS (pre+post) vs CEUS(post))
c) $p = 0.008$ (CEUS (pre+post) vs D-CT)

Micro flow imaging

We attempted to evaluate microvascular changes of various liver tumors using next generation contrast agents such as SonoVue™ and Definity™ and a new contrast technique, Micro Flow Imaging (MFI) by means of morphological changes seen in liver tumors on MFI and histopathological findings. We ultimately aimed to clarify whether this new method could be used for diagnosis of histological differentiation.

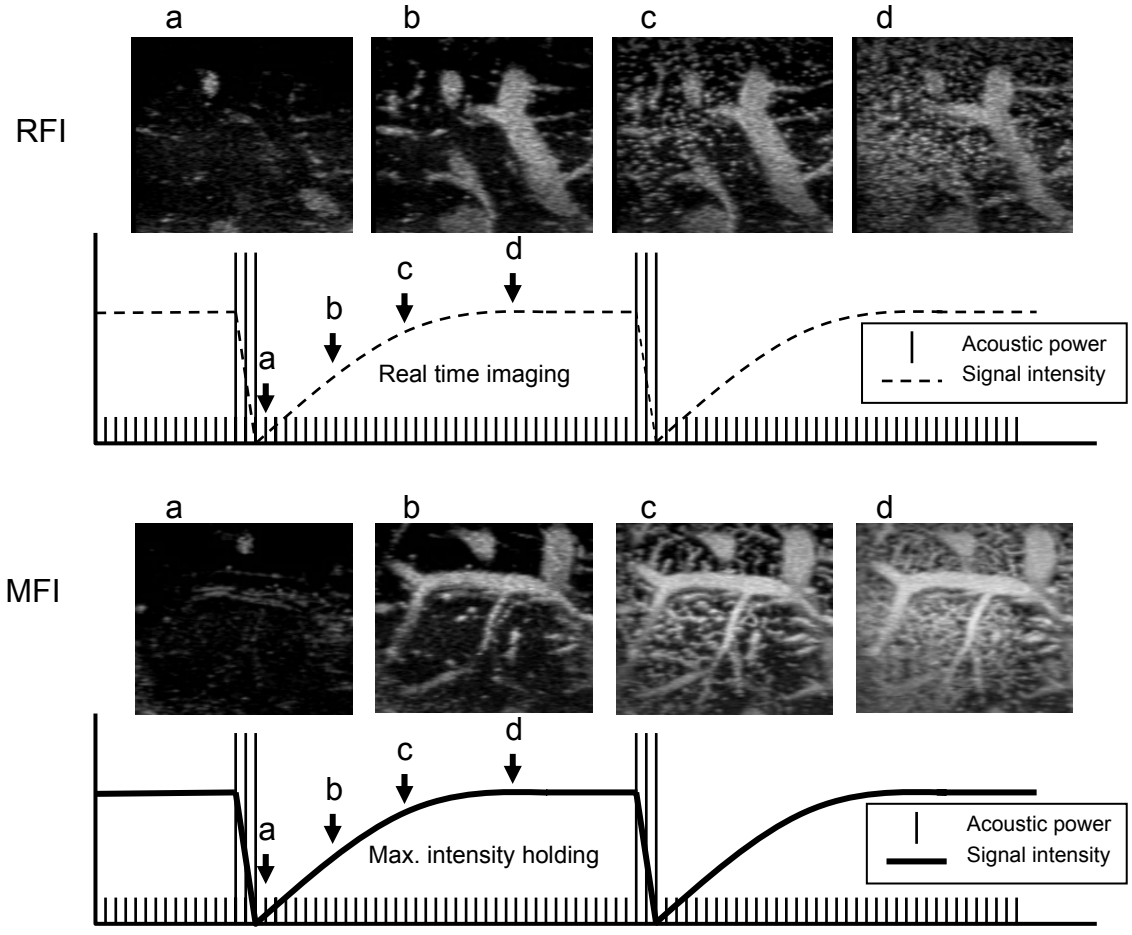

Figure 1. *Schema of flash replenishment imaging (FRI) and micro flow imaging (MFI).*

Figure 2.
Micro flow imaging of hepatocellular carcinoma. Histological diagnosis was poorly differentiated hepatocellular carcinoma.

SonoVue™ (Bracco, Italy) *and* ***MFI mode (Toshiba, Aplio, Tokyo)*** *were used.*

The role of contrast-enhanced ultrasound in pancreatic diseases characterization

Kun Yan, Ying Dai, Yan-Bin Wang, Shan-Shan Yin, Ling Huo, Wei Yang, Hui Zhang, Wei Wu, Min-Hua Chen

Department of Ultrasound, School of Oncology, Peking University, Beijing 100036, China

Objective: To observe the enhancement patterns of pancreatic diseases and evaluate the role of contrast-enhanced ultrasound (CEUS) in pancreatic diseases characterization compared with conventional ultrasound, contrast-enhanced CT (CECT) and biospy.

Material and methods: Eight-one patients with pancreatic diseases underwent CEUS using SonoVue and contrast tuned imaging (CnTI) technique. Of them, 72 patients with final diagnosis including 54 malignant and 18 benign cases were enrolled in this study. Twenty-three cases were diagnosed by operation pathology and 44 by biopsy pathology, the other 5 cases were diagnosed clinically including 3 unresectable malignant cases (with elevated CA 199 level higher than 1000 U/ml) and 2 cases with metastasis in liver and lung. The average size of the lesions was 4.6¡À1.4cm (size range from 1.0 to 10.5cm, median, 4.5cm). The time of the beginning of enhancement, peak enhancement, the beginning of wash-out and the transit time (from the beginning of enhancement to wash-out) of the diseased area and normal pancreatic tissue were analyzed for each case.

Results: The beginning of enhancement of malignant pancreatic diseases was significantly slower than normal pancreatic tissue and the beginning of wash-out time was significantly faster than normal pancreatic tissue, while there was no significant difference between benign pancreatic diseases and normal pancreatic tissue. The transit time of malignant diseases was significantly shorter than benign diseases and normal pancreatic tissue. The most common enhancement pattern of malignant diseases was peripheral enhancement with irregular non-enhanced area inside, while the benign diseases appeared homogeneous enhancement. The diagnostic accuracy of CEUS, CECT and biopsy in pancreatic diseases characterization was 87.5% (63/72 cases), 81.8% (54/66 cases), 92.7% (38/41 cases), respectively, which were all significantly different from that of conventional ultrasound (56.9%, 41/72 cases). But there was no significant difference between CEUS and CECT.

Conclusion: CEUS could afford more information of the vascularization of pancreatic diseases, thus improve the diagnostic ability in pancreatic diseases characterization. The diagnostic accuracy of CEUS is similar to CECT.

Key words: contrast-enhance ultrasound, pancreatic diseases, diagnosis

Evaluation of pericardial hydatid cysts by different echocardiographic imaging modalities

A Nemes, ML Geleijnse, RJ van Geuns, K Caliskan, JS McGhie, OII Soliman, FJ ten Cate

Department of Cardiology, Thoraxcentre, Erasmus MC, Rotterdam, The Netherlands

Cardiac hydatid cyst is a rare complication of parasitic infection caused by Echinococcus granulosus. This case report shows the complementary function of the diverse echo modalities. Two-dimensional transthoracic echocardiography identified two structures, suspected for hydatid cysts. With contrast echocardiography the definite diagnosis of an extra-cardiac structure was confirmed. SonoVue® microbubbles pass the pulmonary circulation and opacify all cavities connected to the heart, so non-opacified structures are identified as extra-cardiac. Real-time three-dimensional echocardiography allowed a more precise evaluation of the cystic size, shape and structure and permitted anyplane analysis.

Application of measuring the changes of haemodynamic parameters of hepatic artery and vein in diagnosis of liver metastases by contrast-enhanced ultrasound

Li AH, Zhou JH, Jiang HH, Chen XX, Liu LZ, Pei XQ, Han F, Chen XY

Cancer Center, Sun Yat-Sen University, Guangzhou, China

Objective To investigate the value of detecting the changes of haemodynamic parameters of hepatic artery and vein in diagnosis of liver metastasis by contrast -enhanced US.

Methods 52 patients with proven liver metastases(study group) and 23 normal volunteers(control group) have been recruited to be studied. Each subject was administrated with bolus injection of SonoVue (Bracco,Milan,Italy). The arrival times in the hepatic artery(AT HA), time to peak in the hepatic artery(TTP HA), peak intensity of the hepatic artery(PI HA), arrival times in the hepatic vein(AT HV), time to peak in the hepatic vein(TTP HV) and peak intensity of the hepatic vein(PI HV) were measured with ACQ Time-Intensity Curve Analysis software (Acuson, Sequoia 512 paregan SIEMENS USA). The hepatic artery to vein transit time(HAVTT) was calculated as the difference between the arrival times in the hepatic artery and the hepatic vein.

Results AT HA, TTP HA, AT HV and TTP HV in study group were shorter than that of control group（$P < 0.01$）. PI HA and PI HV in study group were higher than that of control group（$P < 0.01$）. HAVTT in study group were shorter than that of control group（$P < 0.001$）. The shortening of AT HV and HAVTT caused by hepatic metastases do not correlate with the vascularization of the liver metastases, size and number of the hepatic metastases and the type of primary malignancies.

Conclusions Detecting the changes of haemodynamic parameters of hepatic artery and vein by contrast-enhanced US help to diagnose liver metastases.

Real-time intravenous myocardial contrast echocardiography using low emission power does not induce arrhythmias in healthy volunteers or patient with coronary artery disease

P.A. Dijkmans, C.A. Visser, O.Kamp

Department of Cardiology, VU University Medical Center, Amsterdam, the Netherlands

Introduction Several studies investigated the occurrence of arrhythmias during triggered myocardial contrast echocardiography (MCE), reporting an increased incidence of premature ventricular complexes (PVCs) during end-systolic imaging with high intensity ultrasound. Whether arrhythmias are induced by real-time MCE, using continuous imaging with low emission power and high-energy-ultrasound microbubble destruction (flash), is unknown. The purpose of the study was to assess the occurrence of arrhythmias during real-time MCE in healthy volunteers and patients with known of suspected coronary artery disease (CAD).

Methods 50 healthy volunteers and 18 patients with known or suspected CAD underwent real-time MCE using Sonovue and power pulse inversion (ATL 5000) at rest and during adenosine stress. The frequency of premature atrial- (PACs) and PVCs was analyzed off-line before (baseline) and during MCE (rest and stress) using single lead ECG-monitoring from video-tracings.

Results Incidental flash-related PVCs occurred in healthy subjects. PACs at baseline occurred with a frequency of 0.01±0.07 PACs/min and remained equal at rest (0.02±0.07 PACs/min, P=NS vs. baseline), and stress (0.03±0.13 PACs/min, P=0.11 vs. baseline). The frequency of PVCs at baseline (0.04±0.23 PVCs/min) did not differ from the number of PVCs/min at rest (0.04±0.23, P=NS), and stress (0.03±0.14, P=NS). In CAD-patients, frequency of PACs at rest (0 PAC/min) and stress (0.21±0.63 PACs/min) was not significantly increased compared to baseline (0.05±0.20 PACs/min). The frequency of PVCs at baseline was 0.21±0.63 PVC/min, compared to 0.19±0.61 at rest (P=NS), and 0.23±0.65 at stress (P=NS).

Conclusion Our data demonstrate that real-time MCE does not increase the frequency of premature complexes when using low emission power and high energy ultrasound flashes in healthy volunteers or CAD patients.

Resting detection of high-grade coronary stenosis with preserved local myocardial function in humans.

Jarosław D. Kasprzak, Paulina Wejner-Mik, Piotr Lipiec.

Medical University of Lodz, Bieganski Hospital, Kniaziewicza 1/5, 91-347 Lodz, Poland

We present the clinical cases of patients with high-grade resting coronary stenosis with preserved local myocardial function.

During a resting study, with chest pain absent, qualitative perfusion echocardiogram using Optison demonstrated subendocardial perfusion defects indicating a possibility of coronary flow abnormlaity. the finding was confirmed with coronary angiography.

The current options for resting stenosis assessment as well as absolute perfusion measurement will be discussed.